UNIVERSIDADE FEDERAL DE SANTA CATARINA
CENTRO TECNOLÓGICO (CTC)
PROGRAMA DE PÓS-GRADUAÇÃO EM ENGENHARIA QUÍMICA

Tailin Rieg

Chitosan-Gelatin Beads Containing Copaiba Oil By Nanoemulsion Complex Coacervation

Florianópolis
2022

Tailin Rieg

Chitosan-Gelatin Beads Containing Copaiba Oil By Nanoemulsion Complex Coacervation

Dissertação submetida ao Programa de Pós-Graduação em Engenharia Química da Universidade Federal de Santa Catarina para a obtenção do título de Mestre em Engenharia Química.

Orientador: Prof. Dr. Ricardo Antonio Francisco Machado

Coorientador: Dr. Angelo Oliveira Silva

Florianópolis, SC, Brazil

2022

Ficha de identificação da obra elaborada pelo autor,
através do Programa de Geração Automática da Biblioteca Universitária da UFSC.

Rieg, Tailin
Chitosan-Gelatin Beads Containing Copaiba Oil By Nanoemulsion Complex Coacervation / Tailin Rieg ; orientador, Ricardo Antonio Francisco Machado, coorientador, Angelo Oliveira Silva, 2022.
85 p.

Dissertação (mestrado) - Universidade Federal de Santa Catarina, Centro Tecnológico, Programa de Pós-Graduação em Engenharia Química, Florianópolis, 2022.

Inclui referências.

1. Engenharia Química. 2. Óleo de copaíba. 3. Nanoemulsão. 4. Coacervação complexa. 5. Quitosana. I. Machado, Ricardo Antonio Francisco. II. Oliveira Silva, Angelo. III. Universidade Federal de Santa Catarina. Programa de Pós Graduação em Engenharia Química. IV. Título.

Tailin Rieg

Chitosan-Gelatin Beads Containing Copaiba Oil By Nanoemulsion Complex Coacervation

O presente trabalho em nível de mestrado foi avaliado e aprovado por banca examinadora composta pelos seguintes membros:

Estela Nunes, Dr.ª
EMBRAPA

Tamara Agner Miguez, Dr.ª
Universidade Federal de Santa Catarina - UFSC

Certificamos que esta é a **versão original e final** do trabalho de conclusão que foi julgado adequado para obtenção do título de Mestre em Engenharia Química.

Documento assinado digitalmente
Debora de Oliveira
Data: 03/11/2022 19:19:01-0300
CPF: ***.453.929-**
Verifique as assinaturas em https://v.ufsc.br

Coordenação do Programa de Pós-Graduação

Documento assinado digitalmente
Ricardo Antonio Francisco Machado
Data: 03/11/2022 19:46:53-0300
CPF: ***.377.139-**
Verifique as assinaturas em https://v.ufsc.br

Prof. Ricardo Antonio Francisco Machado, Dr.
Orientador

Florianópolis, 2022.

ACKNOWLEDGMENTS

Firstly, I would like to thank my family, especially my husband, for all their support, incentive, and patience. I always felt them encouraging me to pursue my dreams.

To my advisor, Professor Ricardo A. F. Machado, not only for accepting the challenge of guiding a student that was long away from the university, but mainly for being so kind in welcoming my dream while opening the doors of the academic scene. Walking by your side was a memorable opportunity in my academic trajectory that I won't forget. Thank you for your patience, for your precious time, for your comprehension, and for being an example to be followed.

To my co-advisor, Dr. Angelo Silva, for all his support, and friendship, for foment discussion and listen my opinion, for being a great encourager of my work and a teacher for me.

To Dra. Tamara and Arthur Cordeiro, for the analyses, for the teachings, for the friendship, and for being ever available in the art of help and instruct. You had a great impact on my apprenticeship.

To my colleague and friends in LCP, especially Julia, Manu, and Regi, for all the conversations, exchanges of ideas and for forming a group committed to research development.

To Analysis Center, LABMAT, LCME, and LINDEN for being supported laboratory structure for the development of the present work.

To EQA/UFSC for the university infrastructure and opportunity to develop the research.

To Ministério da Agricultura, Pecuaria e Abastecimento for the opportunity to take a few months off work to focus on this research project.

RESUMO

O óleo de copaíba tem sido amplamente reconhecido por suas propriedades medicinais, especialmente anti-inflamatórias, cicatrizantes e antimicrobianas. No entanto, para o sucesso das aplicações clínicas é necessário superar algumas limitações, como tendência à oxidação, baixa biodisponibilidade e taxa de degradação rápida. Nesse sentido, o desenvolvimento de uma nanoemulsão de óleo de copaíba seguida de encapsulação com coacervados do complexo gelatina/quitosana foi desenvolvido com o objetivo de aumentar a estabilidade e biodisponibilidade do óleo. Primeiramente, o desenvolvimento da nanoemulsão foi avaliado por espalhamento dinâmico de luz (DLS) e aprimorado através da avaliação de diferentes variáveis de processamento. Diâmetro médio de partícula de 281,6 ± 5,813 nm e PdI de 0,293 ± 0,006 foram alcançados após homogeneização a 13.000 rpm por 6 min. A determinação do potencial Zeta foi realizada para avaliar a estabilidade da emulsão. O resultado sugeriu que a gelatina cobriu a superfície das nanocápsulas e legitimou a incorporação adicional de polissacarídeo catiônico para coacervação complexa. A formação de partículas coacervadas foi investigada em três proporções diferentes de quitosana para gelatina (CS:G) (1:15, 1:10 e 1:5) em pH 5,0. Complexos solúveis foram formados a uma razão CS:G de 1:15. Nas condições testadas, a formação de coacervados foi levemente maior na razão CS:G de 1:10 (89%). Os resultados sugeriram a influência da razão mássica dos biopolímeros para o rendimento de coacervação bem como para as morfologias de encapsulamento. Imagens de microscopia óptica e espectros de FTIR indicaram a incorporação de gotículas de óleo de copaíba pelo processo de coacervação, e esferas multinucleadas foram evidenciadas pela primeira análise. O encapsulamento do óleo de copaíba por esferas de coacervados de quitosana e gelatina foi também apontado a partir das imagens obtidas por microscopia eletrônica de transmissão. Assim, este trabalho desenvolveu um sistema de coacervado formado sem o uso de agentes químicos de reticulação como uma abordagem eficiente para encapsulamento de nanoemulsão de óleo de copaíba.

Palavras-chave: óleo de copaíba; nanoemulsão; gelatina; quitosana; coacervação complexa.

RESUMO EXPANDIDO

Introdução

Historicamente, a fitoterapia tem sido utilizada na medicina popular para tratar doenças e restabelecer a saúde, principalmente devido à sua eficiência, baixa toxicidade, biocompatibilidade e baixo custo. O óleo de Copaíba, extraído de árvores do gênero *Copaifera*, destaca-se como um importante extrato terapêutico, especialmente devido a sua atividade anti-inflamatória, cicatrizante, antimicrobiana, larvicida e antineoplásica, já comprovada por estudos farmacológicos (LEANDRO *et al*., 2012). Entretanto, sua utilização pode ser prejudicada por fatores como exposição à luz e ao calor, oxidação, bem como baixa solubilidade em água. Desta forma, o desenvolvimento de estratégias de encapsulamento e incorporação desse material em matrizes mais hidrofílicas apresentam-se como uma importante abordagem para aumento da biodisponibilidade e eficácia de tratamentos.

Surfactantes de baixa massa molar e/ou substâncias macromoleculares anfifílicas são amplamente usadas nos processos de emulsificação, buscando reduzir a tensão interfacial entre as gotas de óleo e mantê-las estáveis (evitando coalescência). Neste sentido, lecitina de soja e gelatina apresentam-se como boas seleções para a elaboração de uma nanoemulsão de óleo de copaíba, pois além de possuírem alta biocompatibilidade e excelentes propriedades emulsificantes, têm demonstrado atividade sinérgica no desenvolvimento de nanoemulsões. Além disso, graças a presença de gelatina na superfície das nanogotas, o controle do pH do meio possibilita a ocorrência de interações eletrostáticas com macromoléculas com cargas opostas, permitindo assim o processo de coacervação complexa com a quitosana. Tal procedimento tende a gerar o recobrimento superficial das nanogotas formadas no processo de emulsificação, aumentando a resistência do material a fatores externos e agregando funcionalidades características decorrentes das interações poliméricas do coacervado.

Objetivo

Neste trabalho foi proposto o desenvolvimento de uma nanoemulsão de óleo de copaíba e posterior coacervação complexa utilizando biopolímeros de quitosana e gelatina, visando aumentar a estabilidade e biodisponibilidade da emulsão. Foram comparadas diferentes proporções de gelatina e quitosana em pH controlado a fim de avaliar o maior rendimento de encapsulação e coacervação.

Metodologia

Para o desenvolvimento das nanoemulsões, diferentes concentrações de óleo de copaíba, lecitina de soja (surfactante selecionado) e gelatina (tipo B) foram testadas, assim como variações de velocidade rotacional e tempo de agitação. A partir dos resultados preliminares, as concentrações dos materiais foram fixadas como sendo: 1% (m/v) de gelatina, 1% (m/v) lecitina de soja e 1% (m/v) óleo de copaíba. As homogeneizações foram realizadas no ULTRA-TURRAX®, com frequências variando de 3.400 a 13.000 rpm, com tempos de 2 a 30 min (a depender do grupo de experimentos realizados). A temperatura foi controlada e mantida em 40 ºC. Para a segunda etapa do trabalho (coacervação complexa), foi selecionado o grupo de experimentos em que a nanoemulsão foi preparada com agitação a 13.000 rpm por 6 min.

Três diferentes concentrações de quitosana foram preparadas para avaliação do processo de coacervação, sendo as proporções de quitosana:gelatina nas razões de: 1:15, 1:10 e 1:5. A concentração de quitosana correspondente foi dispersa em uma solução aquosa (10 mL) de ácido acético glacial (0,3 %v/v) sob agitação magnética à temperatura ambiente por 24 h e então adicionada gota a gota nas dispersões coloidais do respectivo grupo. As soluções foram mantidas sob agitação a 200 rpm por 4 horas e temperatura controlada em 40 ºC. O pH foi avaliado e, caso necessário, corrigido para o valor desejado (pH=5,0). As amostras ficaram em repouso por 24 horas para avaliação do processo de coacervação.

Por fim, os grupos caracterizados pelas diferentes concentrações de quitosana foram estudados, a fim de se verificar o comportamento dos blends de biopolímeros e a subsequente formação de complexos e coacervados. Testes para avaliação do rendimento do processo de coacervação e eficiência da encapsulação, assim como a avaliação das morfologias do coacervados foram realizados (FTIR, MEV, TEM, CY).

Resultados e Discussão

A análise do óleo de copaíba (utilizado nessa dissertação) por cromatografia gasosa com detecção por massa foi efetuada para determinar o perfil de terpenos, aos quais são atribuídas suas propriedades medicinais. Os resultados obtidos estão de acordo com a bibliografia, sendo o β-Cariofileno o componente encontrado em maior proporção (59% aproximadamente).

Ainda sobre a caracterização de materiais utilizados, procedeu-se com a determinação de cargas nas superfícies dos polímeros utilizados no processo de coacervação complexa em função do pH. O ponto isoelétrico da gelatina foi atingido no pH 4,8, a partir do qual cargas negativas são detectadas com o aumento do pH. Assim, e considerando que a quitosana utilizada apresentou cargas positivas em toda a faixa de interesse, com maior valor de potencial Zeta para o pH 5,0, estabeleceu-se que esta seria a faixa ideal para ser aplicada no processo de coacervação complexa entre os referidos biopolímeros.

Todas as formulações para estudo da distribuição do tamanho de partícula para as nanoemulsões de óleo de copaíba foram analisadas via espalhamento dinâmico de luz (DLS). Para velocidades de agitação inferiores a 8.000 rpm, o equipamento não detectou formação de partículas, as quais provavelmente ainda estavam com dimensões muito extensas devido ao pequeno tempo de agitação. Ao analisar os resultados obtidos para os testes em 8.000 rpm, o aumento de tempo de homogeneização acarretou uma importante melhora na diminuição da polidispersão das emulsões. Uma amostra menos polidispersa (PDI = 0,369 ± 0,064) e com menores tamanhos de partículas (370 ± 4,869 nm) foi obtida quando se mantiveram as condições de homogeneização e aumentou-se a concentração do óleo de copaíba e da lecitina de 0,5% (m/v) cada para 1% (m/v) cada. Um efeito semelhante já foi descrito na literatura para nanoemulsões desenvolvidas com gelatina e lecitina de soja (XUE; ZHONG, 2014). Ao elevar-se a velocidade de agitação para 11.500 rpm, uma significativa diminuição no diâmetro das partículas foi alcançada (281,3 ± 4,557 nm, PDI = 0,317 ± 0,010). Ainda que muitos estudos indiquem que o aumento da velocidade e do tempo de agitação proporcionem melhores resultados no desenvolvimento de nanoemulsões, observou-se um comportamento distinto. Testes a 13.000 rpm apontaram um aumento no tamanho das gotas e maior polidispersão em tempos de agitação acima de 10 min. Por fim, o melhor resultado foi obtido para agitação a 13.000 rpm por 6 min, denominado grupo T9, o qual foi selecionado para dar prosseguimento ao trabalho. O potencial Zeta da amostra foi avaliado (-13,067 mV) sugerindo que a gelatina estava encapsulando as nanogotas de óleo.

Através da técnica de FT-IR foi possível verificar que o óleo de copaíba foi incorporado no coacervado, assim como a lecitina de soja, a gelatina e a quitosana. A microscopia óptica foi outra técnica empregada para conferir a estrutura dos coacervados. As imagens sugerem que formas esféricas de tamanho reduzido se aglomeraram nos três grupos analisados, assim como indicam a presença de envoltórios. O grupo com maior quantidade de quitosana demonstrou maior tendência a formar associações mais densas, como uma espécie de estrutura com muitos núcleos. O encapsulamento do óleo de copaíba por esferas de coacervados de quitosana e gelatina foi também apontado nas imagens obtidas por microscopia eletrônica de transmissão.

Os testes de rendimento de coacervação indicaram que complexos solúveis foram formados para o grupo CS:G 1:15 nas condições testadas, o que provavelmente se deve a pequena quantidade de quitosana e consequente menor quantidade de íons por unidade de volume de solução. Uma pequena diferença na formação de coacervados foi observada na razão CS:G de 1:10 (89 %) em comparação com a razão CS:G de 1:5 (88 %). Acredita-se que este resultado pode estar relacionado ao fato de que o sistema um pouco mais diluído proporcionou mais espaço e facilitou o desdobramento e a interação adequados da CS (molécula de tamanho grande) com a gelatina. Portanto, a mobilidade favoreceria as cadeias de biopolímeros para alcançar conformações adequadas para a formação de complexos.

Considerações Finais

O desenvolvimento de nanoemulsão de óleo de copaíba e posterior coacervação complexa utilizando os biopolímeros quitosana e gelatina foram realizados com sucesso. Este sistema consiste em uma abordagem eficiente para melhorar as aplicações farmacêuticas do referido óleo. Gelatina e lecitina de soja foram utilizadas como agentes emulsificantes no desenvolvimento da nanoemulsão, proporcionando a formação de nanogotas com tamanhos de até 281.6 ± 5.813 nm.

O maior rendimento de coacervação foi encontrado no grupo CS:G de 1:10, enquanto no grupo CS:G 1:15 não houve separação de fases (precipitação) após finalização do processo. Análises realizadas sugerem a influência da razão mássica dos biopolímeros para o rendimento de coacervação bem como para as morfologias de encapsulamento.

Palavras-chave: óleo de copaíba; nanoemulsão; gelatina; quitosana; coacervação complexa.

ABSTRACT

Copaiba oil has been widely recognized for its therapeutic properties, especially anti-inflammatory, wound healing, and antimicrobial activities. However, clinical applications success must overcome some physical barriers such as oxidation tendency, low bioavailability, and rate of degradation. In this regard, the development of copaiba oil nanoemulsion followed by encapsulation with gelatin/chitosan complex coacervates was developed aiming to increase the oil encapsulation stability and bioavailability. Firstly, nanoemulsion development was performed and improved through the evaluation of different processing variables by dynamic light scattering (DLS). Mean particle diameter of 281.6 ± 5.813 nm and PdI of 0.293 ± 0.006 were achieved after homogenization at 13.000 rpm for 6 min. Zeta-potential evaluation was performed to assess emulsion stability. The result suggested that gelatin covered the surface of nanocapsules and legitimate further incorporation of cationic polysaccharide for complex coacervation. Coacervated particles formation was investigated at three different chitosan to gelatin (CS:G) ratios (1:15, 1:10, and 1:5) at pH 5.0. Soluble complexes were formed at a CS:G ratio of 1:15. In the conditions tested, the coacervate formation was slightly higher at the CS:G ratio of 1:10 (89%). Results suggested the influence of biopolymers mass ratio on coacervation yield and encapsulation morphologies. Optical microscopy images and FTIR spectra indicated the incorporation of copaiba oil droplets via the coacervation process, and multinucleated beads were evidenced by the former analysis. The transmission electron microscopy confirms successful encapsulation of copaiba oil by chitosan and gelatin complex coacervation beads. In summary, this work developed a coacervate system formed without the use of chemical crosslinking agents as an efficient approach for encapsulation of copaiba oil nanoemulsion.

Keywords: copaiba oil; nanoemulsion; gelatin; chitosan; complex coacervation.

LIST OF FIGURES

LIST OF TABLES

LIST OF ABBREVIATIONS

CO	Copaiba oil
CS	Chitosan
CY	Coacervation yield
DD	Degree of deacetylation
DLS	Dynamic light scattering
ECM	Extracellular matrix
EI	Electron Impact Ionization
EQA	Department of Chemical Engineering and Food Engineering
FT-IR	Fourier Transform Infrared
GC/MS	Gas chromatography/mass spectrometry
G	Gelatin
GAGs	Glycosaminoglycans
GB	Type B gelatin
GC	Gas Chromatography
HA	Hyaluronic acid
HCl	Hydrochloric acid
HPLC	High-performance liquid chromatography
Ip	Isoelectric point
KBr	Potassium bromide
KOH	Potassium hydroxide
LMWE	Low molecular weight emulsifier
LRI	Linear retention index
MIC	Minimum inhibitory concentration
MM	Molar mass
NaOH	Sodium hydroxide
NIST	National Institute of Standards and Technology
OM	Optical microscopy
o/w-NE	Oil-in-water nanoemulsions
PdI	Polydispersity index
SL	Soy lecithin

TEM	Transmission Electron Microscopy
UFSC	Federal University of Santa Catarina
WHO	World Health Organization
Zp	Zeta potential

TABLE OF CONTENTS

1 INTRODUCTION

1.1 MOTIVATION

Historically, medicinal plants have been used in folk medicine to treat diseases and restore health especially due to their efficiency, low toxicity, biocompatibility, and low cost (MENEZES *et al*., 2022). Since 2002, the World Health Organization (WHO) has recognized the importance of traditional medicine as a part of healthcare (RICARDO *et al*., 2018). In this scenario, copaiba oil stands out as a widely used therapeutic agent, characterized as a medicinal plant of interest according to the Brazilian Health Ministry (BRAZIL, 2021).

Copaiba oil is mainly extracted from tree species of the genus *Copaifera*, found mainly in the Brazilian amazon rainforest, containing mixtures of sesquiterpenes and diterpenes, whose composition may vary between plant species (DIAS *et al*., 2014). Beyond various ethnopharmacological indications of oleoresins extracted from these plants, some of them have been confirmed by pharmacological studies: anti-inflammatory, wound healing, antimicrobial, antileishmanial, larvicidal, and antineoplastic activities (LEANDRO *et al*., 2012). Copaiba oil is widely used in folk medicine to act against several illnesses and combat various kinds of pathogens, comprising a good alternative for targeting antibiotic resistant microorganisms (MARANGON *et al*., 2017).

However, several obstacles generally restrict the benefits linked to this bioactive oil. Toxic compounds can be formed from vegetable oils oxidation, that may largely affect biological tissues. Numerous studies have evidenced that this class of oil is unstable and degraded easily without protection from external factors, being subjected to volatilization, heat loss, and light damage (LAMMARI *et al*., 2021). Moreover, the intense aroma, water-insoluble nature, and low bioavailability of copaiba oil assets the limitation of clinical practice application (MARANGON *et al*., 2017).

For all those reasons presented, designing suitable carriers by using an encapsulation approach is an interesting method to overcome outlined restrictions of Copaiba oil and provide improved biomedical applications (LAMMARI *et al*., 2021). Emulsification technology is a key step in the encapsulation of oils, which are generally applied for bioactive enclosement in aqueous solutions (BAKRY *et al*., 2016). Some advantages of these systems are relative ease of preparation, low cost, and aid to sustain the oil or lipid against oxidation and vaporization, among others (ROY *et al*., 2017). To increase the stability of emulsions, low-molecular-weight surfactants or amphiphilic macromolecular substances are used to decrease interfacial tension

(ZHANG *et al*., 2020b). In this sense, soy lecithin stands out as a widely used surfactant in the biotechnology industry, presenting high biocompatibility and excellent emulsifying property mainly attributed to phospholipids presented in their backbone structure (VATER *et al*., 2022; XUE; ZHONG, 2014).

Previous studies have successfully produced oil-in-water nanoemulsions based on soy lecithin and gelatin blends (LI *et al*., 2020; XUE; ZHONG, 2014; ZHANG *et al*., 2020b). This strategy of nanoemulsification presents attractive perspectives. The nanometric size of the droplets allows high contact surface and uniform distribution of compounds when in contact with human tissues (BOUCHEMAL *et al*., 2004). Furthermore, enables the incorporation of an oil with an unctuous character in a more acceptable hydrophilic formulation, providing reduced side effects and increased skin penetration (DIAS *et al*., 2014).

Complex coacervation has been broadly used as an effective method for micro/nanoencapsulation, able to enhance nanoemulsions stability through an appropriate choice of compounds (GONZÁLEZ-MONJE *et al*., 2021; MU *et al*., 2022; TIMILSENA *et al*., 2019). Complex coacervates are formed by maximizing favorable interactions among different types of macromolecules (association), such as polyelectrolytes of opposite charge (NAKASHIMA; VIBHUTE; SPRUIJT, 2019). In the presence of colloidal dispersions (*e.g.* oil-in-water emulsion), the coacervates distributes on the interface, forming a uniform coating, which jellifies upon cooling, improving the yielding of capsules (GONZÁLEZ-MONJE *et al*., 2021).

Beyond various biopolymers that can be used in complex coacervation, gelatin in association with other polysaccharides has remained the most widely employed protein source, due to its excellent structural and functional properties (TIMILSENA *et al*., 2019). Natural polymers are attractive options mainly due to their similarities with the extracellular matrix, chemical versatility, and inherent cellular interactions (XUE; DAVIDSON; ZHONG, 2017). Additionally, biopolymers such as proteins and polysaccharides in the complexed form are particularly interesting as materials for encapsulation due to their biocompatibility, biodegradability, and improved mechanical strength when compared to individual biopolymers (LIANG *et al*., 2022; ROY *et al*., 2018; TIMILSENA *et al.,* 2017).

In the last decades, there has been significant development of research involving the use of chitosan (CS) and Gelatin (G) as forming materials in the encapsulation of liposoluble liquid core (ROY *et al*., 2018). Chitosan is one of the most widely studied biocompatible amino-

polysaccharide, obtained by alkali-induced de-N-acetylation of chitin, which is a byproduct derived from the exoskeleton of invertebrates (HARISH PRASHANTH; THARANATHAN, 2006). Additionally, exhibits potential applications in various fields such as pharmaceutical, biotechnological, medicinal, and drug-carrier (CHOWDHURY *et al*., 2022). CS shows excellent coagulation and flocculation properties, being capable of interacting with negatively molecules of charged proteins due to the high density of amino groups (KOŁODZIEJSKA *et al*., 2021). In this sense, chitosan coating could improve the stability of complex coacervated capsules in harsh environments, which might have a broad prospect to protect oil droplets against severe harsh environmental stresses (LI *et al*., 2022a).

Therefore, the novelty of the work was to develop copaiba oil nanoemulsion by a binary surfactant system consisting of soy lecithin and gelatin. A second process step regarding the complex coacervation process of the applied protein and chitosan was assayed. This study is important for exploring the potential application of CS and G complex in the encapsulation of lipophilic bioactive components.

1.2 RESEARCH OBJECTIVES

1.2.1 General Objective

This work has the general objective of the development of a copaiba oil nanoemulsion and subsequent complex coacervation using chitosan and gelatin biopolymers, aiming to provide a stable and controlled oil nanoencapsulation process with a coacervated containing a higher bioavailability.

1.2.2 Specific Objectives

The specific objectives of this work are:

a) Produce a copaiba nanoemulsion from a binary surfactant system of gelatin and soy lecithin, evaluating the influence of homogenizing time and speed for copaiba oil nanoemulsion development.

b) Evaluating the developed nanoemulsion proprieties according to the droplet size and colloidal stability for further selection for the coacervation process;

c) Develop a coacervation process with different biopolymers ratios under specific pH values, aiming to ensure proper encapsulation of copaiba oil nanoemulsion;

d) Assess the final coacervated characteristics according to surface morphology, chemical composition, and coacervation process yield.

2 LITERATURE REVIEW

In this chapter, the scientific aspects related to the subjects of the present work that are available in the literature will be addressed. This literature review is divided into different parts to systematize the information, which is related to relevant works on chitosan, gelatin, and the combined use of these biopolymers, encapsulation and coacervation methods, copaiba oil, and emulsion.

2.1 CHITOSAN

Chitosan is one of the most abundant and promising biopolymers, obtained from the partial deacetylation of a natural polymer: the chitin (PEREDA *et al*., 2011). Chitosan has been reported to have a number of functional properties and exhibits innumerable applications in a wide range of fields such as agriculture, packaging, food biotechnology, medicinal and pharmaceutical areas (CHOWDHURY *et al*., 2022; HARISH PRASHANTH; THARANATHAN, 2006).

Structurally, chitosan is a linear polysaccharide consisting of β(1 → 4) linked D-glucosamine residues with a variable number of randomly located *N*-acetyl-glucosamine groups (SUH; MATTHEW, 2000) as presented in Figure 1. It is a polycationic polymer that contains one amino or acetamido group and two hydroxyl groups in the repeating hexosaminide residue, allowing chitosan to be chemically modified to obtain derivatives with improved functionalities and properties (AGRAWAL; STRIJKERS; NICOLAY, 2010; SIVASHANKARI; PRABAHARAN, 2016).

Figure 1 – Chemical structure of chitosan containing the amino, acetamido, and hydroxyl groups.

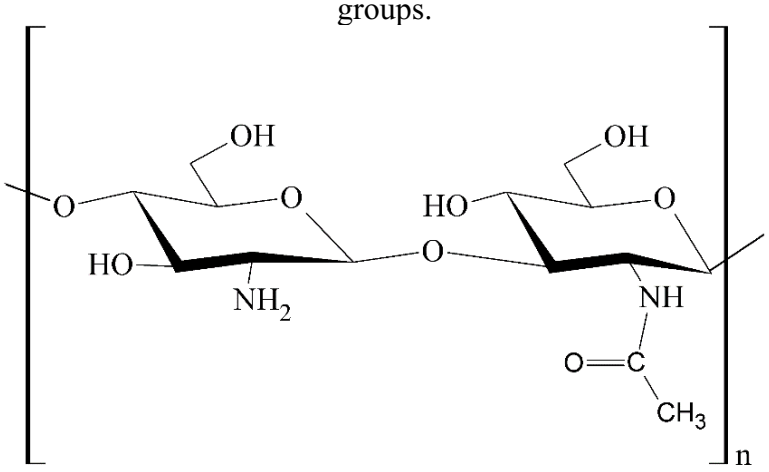

Ref: Author (2022).

2.1.1 Chitin and chitosan production

The precursor in chitosan production is chitin, which is also a linear polysaccharide and considered one of the substances with the highest production rate and biodegradability properties existing in nature (MUXIKA *et al.*, 2017). Chitin is commonly found in invertebrates, as crustacean shells or insect cuticles, but also in some mushroom's envelopes, green algae cell walls, and yeasts (CROISIER; JÉRÔME, 2013).

Despite chitin being abundant and having exceptional functional features such as biocompatibility, bioactivity, biodegradability, and high mechanical strength, it possesses limited application mainly due to the poor solubility in common solvents (DASH *et al.*, 2011). For that reason, the chitosan production from chitin material has a commercial interest (PAKIZEH; MORADI; GHASSEMI, 2021). The major derivative of chitin is chitosan, and the obtaining procedure for these materials is presented in Figure 2.

Figure 2 – The standard chemical extraction processes of chitin and chitosan.

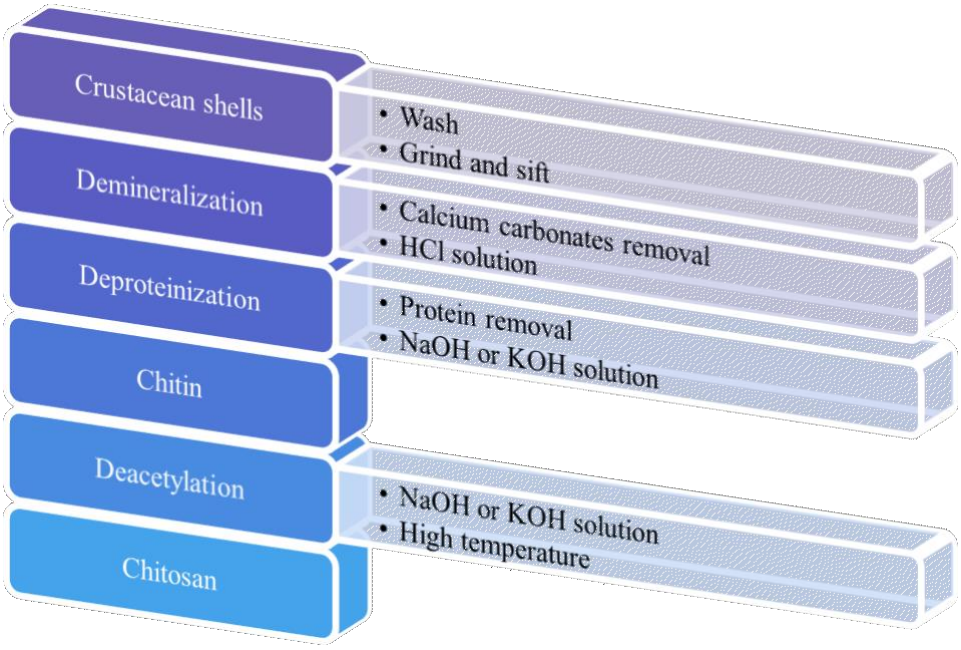

Ref: Author (2022).

As pictured in Figure 2, crab and shrimp shell exoskeleton wastes are the raw material source of biomass for the industrial production of chitin and chitosan (SILVA *et al.*, 2021). After washing, grinding and sieving of raw shell wastes, the resulting material undergoes a demineralization or decalcification process, which involves the removal of calcium carbonates

by acid treatment. Dilute hydrochloric acid (HCl) solution reacts with exoskeleton components (mainly calcium carbonate and chloride), and the obtained material is filtered, washed, and dried (HOSSAIN; MALLIK; RAHMAN, 2020).

The deproteinization process consists of an alkaline treatment aiming to remove proteins, traditionally by treating with sodium hydroxide (NaOH) or potassium hydroxide (KOH) solutions (HUQ *et al*., 2022). If a colorless product is required, a bleaching/decoloration step is added as an additional step, and an organic solvent (like acetone) eliminates pigments such as melanin and carotenoids (PAKIZEH; MORADI; GHASSEMI, 2021).

After chitin extraction, the deacetylation is conducted by chemical hydrolysis of the acetamide groups, normally conducted by strong alkaline treatment (NaOH or KOH) under high temperature and controlled pressure (CROISIER; JÉRÔME, 2013; HUQ *et al*., 2022). When the fraction of glucosamine units surpasses above 50% then it is produced the chitosan and this number of glucosamine units is then denominated as the degree of deacetylation (DD) (HOSSAIN; MALLIK; RAHMAN, 2020).

The experimental conditions applied for deacetylation determines the polymer molar mass (MM) and DD (DASH *et al*., 2011). DD is the most important parameter affecting potential industrial applications of chitin and chitosan, controlling solubility, chemical reactivity during chemical modifications, and biodegradability (MATI-BAOUCHE *et al*., 2014).

2.1.2 Physicochemical and biological properties

The presence of amino groups in the chitosan structure differentiates chitosan from chitin, providing to this polymer several peculiar properties (CROISIER; JÉRÔME, 2013). The amino groups of the D-glucosamine residues enable solubility in diluted acidic aqueous solutions (pH < 6) by NH_2 protonation, attributing polyelectrolyte properties (PAKIZEH; MORADI; GHASSEMI, 2021). In this regard, the protonated amino groups become a polycation that can subsequently form ionic complexes with a wide variety of natural or synthetic anionic species, such as lipids, proteins, and DNA (CROISIER; JÉRÔME, 2013). Regarding biomedical applications, the positively charged amino groups in the chitosan structure confer to this biomaterial mucoadhesive and hemostatic features, with the ability to bind cell membranes (ORYAN; SAHVIEH, 2017).

As mentioned, the presence of the amino groups indicates that pH substantially alters the charged state and properties of chitosan (Figure 3) (DASH *et al*., 2011). Yi *et al*. (2005)

explained that at low pH amines are protonated and positively charged, and chitosan is a water-soluble cationic polyelectrolyte; at high pH (above about 6.5), chitosan's amines become deprotonated and the polymer loses the electrostatic charge and becomes nearly insoluble.

Figure 3 – Schematic illustration of the charged state and properties of chitosan.

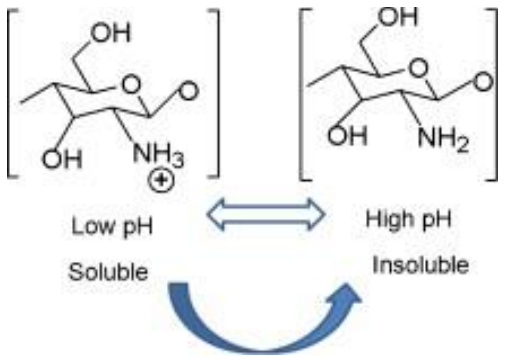

Ref: Adapted from Dash *et al.* (2011).

The degradation rates seem to be affected by DD, degree of crystallinity, distribution of acetyl groups, and length of the chains (DASH *et al*., 2011). About degradation of chitosan inside of the human body, it occurs predominantly by hydrolytic degradation by lysozymes, aided by certain bacterial enzymes in the colon. These mechanisms allow this polysaccharide to be sufficiently excreted (DASH *et al*., 2011; KALANTARI *et al*., 2019). A high degree of deacetylation and molar mass retard CS's biodegradation rate (ORYAN; SAHVIEH, 2017). Relations between DD and a range of physicochemical properties are schematized in Figure 4.

This polysaccharide has extraordinary biological properties. It is a biodegradable, biocompatible, bioactive, non-toxic, non-expensive, and non-immunogenic polymer, with antibacterial and antioxidant capability (AGRAWAL; STRIJKERS; NICOLAY, 2010). The mechanism of the antimicrobial activity of CS is claimed to be related to the positive charge on the NH_3^+ group of the glucosamine monomer at pH < 6.3, which allows interactions with negatively charged microbial cell membranes that lead to the leakage of intracellular constituents (LIU *et al*., 2004).

Beside this mechanism, Pakizeh, Moradi and Ghassemi (2021) also pondered that CS antibacterial and antifungal activities involves its ability to bind to cell DNA via protonated amino groups causing inhibition of the microbial RNA synthesis. Cytocompatibility, hemostatic action, and wound-healing stimulation also mark this natural biopolymer as an

attractive option for biomedical and pharmaceutical fields, capable of interact with the surrounding biological environment without adverse impacts on the host body (HOSSAIN; MALLIK; RAHMAN, 2020; ORYAN; SAHVIEH, 2017).

Figure 4 – Deacetylation degree (DD) influence on CS physicochemical properties.

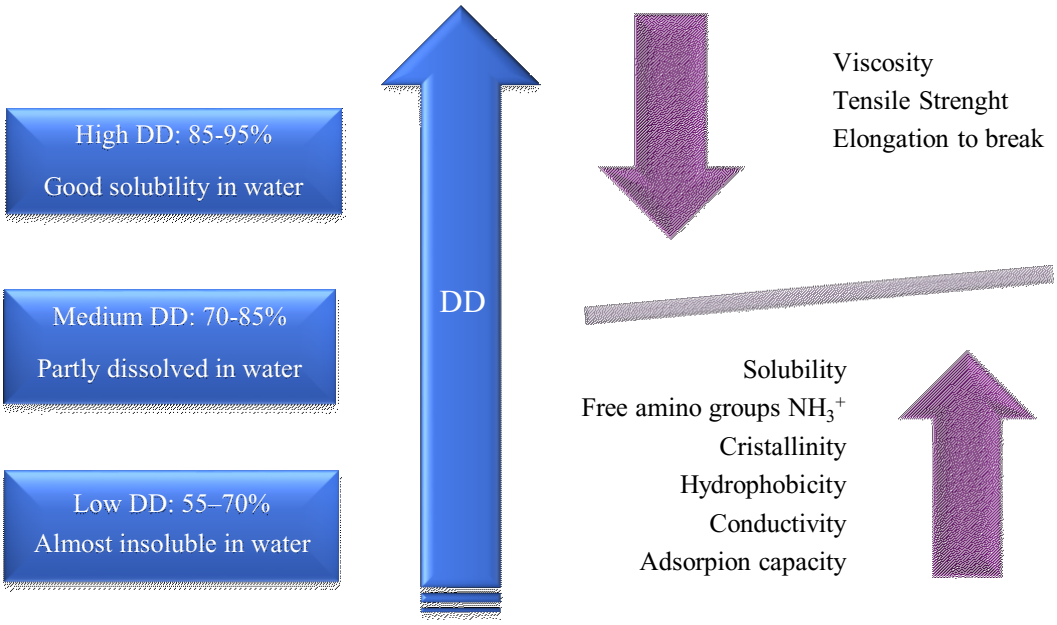

Ref: Adapted from Kolodziejska *et al*. (2021).

CS exerts its wound healing effect by several well-studied mechanisms, including antimicrobial activity, free radical scavenging activity, and regulating the inflammatory response (LOO *et al*., 2022). It can bind to the red blood cells to facilitate clot formation, promoting fibroblast proliferation and increasing the synthesis of natural hyaluronic acid (HA) in the wound region (ORYAN; SAHVIEH, 2017). The ability of CS to support cell attachment and proliferation is related to the structural and chemical properties of the polysaccharide backbone of chitosan that is structurally similarity to glycosaminoglycans (GAGs), the major component of the extracellular matrix of bone and cartilage (ECM) (MAGANTI *et al*., 2011).

CS-based materials are reported as capable of controlled delivery of the loaded molecules or growth factors in the injured area, important characteristics for tissue engineering and regenerative medicine (ORYAN; SAHVIEH, 2017). Ma *et al*. (2017) developed chitosan-based membranes containing antibacterial drugs for wound healing. Biodegradation results demonstrated that the obtained membranes had relatively long-term stabilities and were capable

of drug-controlled delivery with good properties of delayed release, especially for water-insoluble drugs.

The presence of amino groups in the polysaccharide backbone of CS can ionize in acidic pH and interconnect, leading to the formation of 3D crosslink film material, which is an emerging platform for treating different skin disorders like burning, inflammation, and wound (CHOWDHURY *et al*., 2022). This route allowed a localized therapeutic effect by controlling the release of loaded therapeutics.

As the only nature derived cationic polysaccharide, CS can improve emulsion stabilization through combination with anionic species and increase solution viscosity (ROY *et al*., 2017). In this circumstance, chitosan and gelatin blends stand out as an interesting option for encapsulation purposes, which will be discussed in more detail in section 2.4.

In brief, chitosan has exceptional functional properties that make it a unique material for a wide range of applications in areas of great technological impact. Possessing distinguished biological features, this polysaccharide has been extensively used in the medical field, such as in the production of cellular scaffolds, wound healing, and drug administration, among others (MATI-BAOUCHE *et al*., 2014; REZAEI *et al*., 2021). Biodegradability, formidable biocompatibility, antibacterial activity, and low toxicity are the main qualities that support this notoriety.

2.2 GELATIN

Gelatin is a biopolymer widely explored pure or in composite materials for several types of applications such as tissue engineering scaffolds, pharmaceutics, adhesives for wound healing, and drug delivery, among others (NIEHUES; QUADRI, 2017). Gelatin is defined as a heterogeneous mixture of peptides derived from collagen, one of the high-molar mass proteins, containing glycine (around 30 wt. %) and proline/ hydroxyproline (25 wt. %) as the most prominent amino acids (LIU *et al*., 2015; ROY *et al*., 2017). In gelatin, the amino acid composition as well as the sequence differs from one source to another, though always comprising non-polar and polar amino acids (SU; WANG, 2015).

2.2.1 Gelatin production

Gelatins are important natural amphiphilic macromolecules extracted from different animal sources/organs by different extraction methods/parameters (*e.g.* acid, alkali, and enzyme

treatments, extraction temperature, extraction time) (ZHANG *et al.*, 2020d). Produced commercially by partial hydrolysis of collagen, which is the major component of the connective tissues like skin, tendon, and bone, among others (SU; WANG, 2015; TIMILSENA *et al.*, 2019). This process involves breaking the collagen triple-helix molecule, which is stabilized by interchain hydrogen bonds and covalent crosslinks, into a random coil to produce gelatin (GIOFFRÈ *et al.,* 2012). Depending on the hydrolysis conditions, two types of gelatins are obtained, as pictured in Figure 5.

Figure 5 – Different extraction treatments and the obtained types of gelatins.

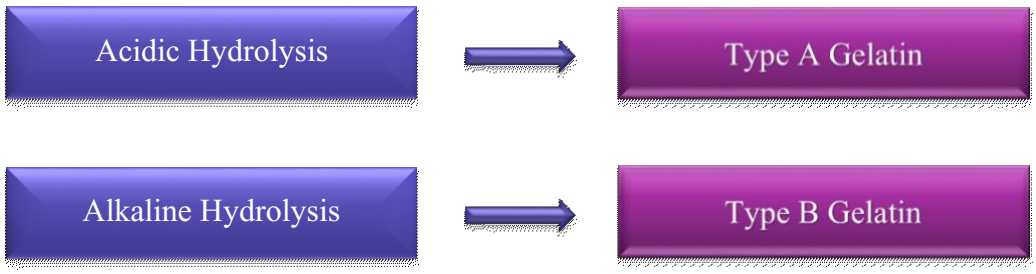

Ref: Author (2022).

The gelatin obtained from the acid extraction process (type A) has a high isoelectric point (Ip) at pH 8 − 9, while gelatin derived from alkaline hydrolysis (type B) has a lower Ip around pH 4 − 5 (ZHANG *et al.*, 2020d). Ip is the pH value at which a gelatin molecule is neutral in charge (AHMADY; ABU SAMAH, 2021a). For pH values higher than its Ip, gelatin has negative charges; for pH values lower than its Ip, gelatin has positive charges (AHMADY; ABU SAMAH, 2021a).

2.2.2 Physicochemical and biological properties

Obtention parameters (*e.g.* pH, temperature, time, and raw material) significantly affect the molecular weight and amino acid compositions of gelatins, characteristics that generate influence on biopolymeric molecular structures, physiochemical and functional properties (ZHANG *et al.*, 2020c, 2020d).

Bloom strength is an important property of gelatin that reflect the average molecular weight of its constituents, being an indicator of the strength and stiffness of a gelatin gel (AHMADY; ABU SAMAH, 2021a). Gel strengths of commercial gelatins are expressed

through bloom values, which is defined as the weight in grams that is required for a specified plunger to depress the surface of a standard gel to a defined depth under standard conditions (KARIM; BHAT, 2009).

Gelatin normally dissolves in water at temperatures above 40 °C, where it exists essentially as isolated, flexible, and usually lightly cross-linked chains, adopting a random coil conformation in solution (SEGTNAN; ISAKSSON, 2004). Below the helix-coil transition temperature, chains start to coil around each other and reform only partially a collagen-like triple helix (COPPOLA; DJABOUROV; FERRAND, 2012). If the gelatin concentration is higher than its critical overlap concentration, molecules will assemble into a network of triple helices to form a thermoreversible viscoelastic gel on cooling (ZHANG *et al*., 2020d).

Owing to their surface-active properties, gelatins can act as an emulsifier in oil-in-water emulsions, an ability that comes from the hydrophobic regions on the protein chains (ZHANG *et al*., 2020d). However, their use in combination with other surfactants is necessary to improve emulsification effectiveness, because gelatin is considered a weak emulsifier and often produces relatively large droplet sizes during homogenization (KARIM; BHAT, 2009). Surfactants and gelatin can interact to form complexes in water (ZHANG *et al*., 2020a). Li *et al*. (2020) achieved an effective oil encapsulation co-emulsified by a complex of gelatin and lecithin, which greatly restricted the migration and losses of oil. Zhang *et al*. (2020a) evaluated interactions between gelatin and four different surfactants to stabilize fish oil emulsions, reporting that surfactant type and preparation pH considerably affect droplet and creaming stability of the systems.

Among various biopolymers that can be used in complex coacervation, gelatin has remained the most widely employed protein source due to its excellent structural and functional properties (TIMILSENA *et al*., 2019). Gelatin molecules and polysaccharides (as chitosan) can form complexes and coacervates, which mostly originate from electrostatic and hydrogen bond interactions between these oppositely charged macromolecules, improving gelation and rheological properties of the systems (HUANG *et al*., 2019). Chemical modification of gelatin further allows for enhanced drug stabilization and higher drug entrapment efficiency (SU; WANG, 2015).

Relatively low cost compared with other proteins, gelatin has broad advantages for biomedical applications, such as high biocompatibility, biodegradability, cell adhesion, accessible functional groups that allow chemical modifications, low immunogenicity, and off-

the-shelf availability (SU; WANG, 2015; TIMILSENA *et al*., 2019). This biopolymer has excellent film-forming properties and is commonly used as coating material in encapsulates (GARCÍA-MORENO *et al*., 2018). In this regard, produced films from gelatin have shown good barrier properties to gases, volatile compounds, oils, and UV light (LI *et al*., 2020). Its physicochemical features, in particular the tunable cross-linking density, degradation kinetics, and gelling properties offer high versatility for the design of drug delivery vehicles (SU; WANG, 2015).

2.3 CHITOSAN AND GELATIN BLENDS

Besides chitosan and gelatin demonstrating noteworthy proprieties, these biopolymers have also drawn the attention of the scientific community in the last decades by their shaping and chemical modification possibilities (AHMADY; ABU SAMAH, 2021b; HUO *et al*., 2018). Beyond their unique structures and interesting characteristics already discussed, these versatile materials can form composites with improved mechanical and thermal properties compared to the individual biopolymers (ROY *et al*., 2018). Figure 6 illustrates this potential. Additionally, due to increased customer consciousness, environmental and health awareness, the production of functional and bio-based products has become an emerging field (SINGH; SHEIKH, 2022).

Figure 6 – Improved characteristics of chitosan-gelatin blends.

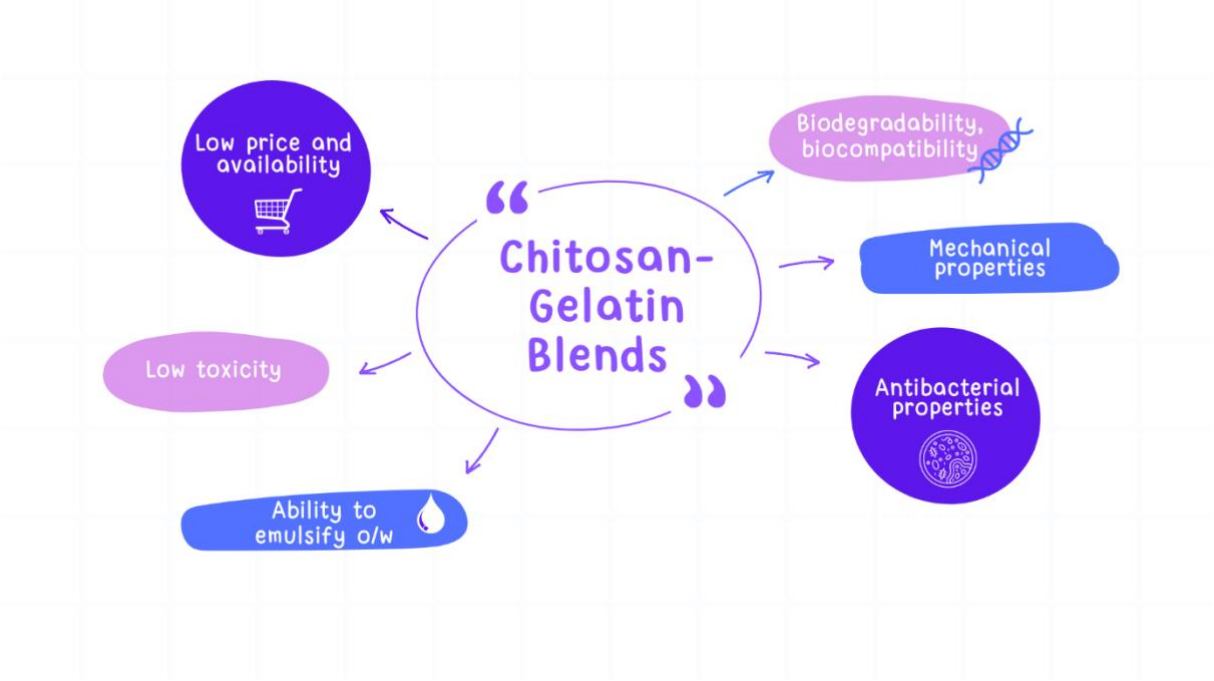

Ref: Author (2022).

When proteins and polysaccharides are dispersed together in an aqueous phase, there are generally three possible potential outcomes: remain dispersed, associate into complexes that remain dispersed, or separate into two phases (also known as coacervation when polymers interact and separate into polymer-rich and polymer-poor phases) (WAGONER; VARDHANABHUTI; FOEGEDING, 2016). Protein/polysaccharide complex systems, mainly generated by electrostatic interactions between oppositely charged macro-molecules, have received increasing interest in recent years (WANG; WANG; HEUZEY, 2016).

CS/G complexes must be developed in some specified pH region, which has been proven as effective Pickering emulsifiers, benefitting the formation of smaller emulsion droplet sizes, successfully hindering droplet coalescence, and increasing emulsion long-term stability (WANG; HEUZEY, 2016). Effective encapsulation technology, able to protect the core material and stabilize functionality, has also been explored by the combination of chitosan and gelatin (AL-MAQTARI *et al*., 2022).

Qiao *et al*. (2017) quoted ionic interaction that can occur between negative charged carboxyl groups in gelatin with the oppositely charged amino groups on the CS chains; furthermore, explained that gelatin also has a large number of polar groups (such as –COOH, $–NH_2$ and –OH groups), capable of forming hydrogen bonds with the –OH and $–NH_2$ groups on the chitosan chains.

In this regard, the combined use of chitosan and gelatin as polymeric blends allow the development of new materials with great merits and improved features for applications in a wide range of industries. Table 1 demonstrates this potential.

Table 1 - Chitosan and gelatin as matrix materials for encapsulation purposes.

Application field	Encapsulated material	Material type	Improved properties	Reference
Food-packaging	3-phenylacetic acid	Nanofiber	Water vapor permeability and antibacterial properties.	(LIU *et al*., 2021)
Food-packaging	Active compounds	Film	Uniform distribution of the actives.	(PÉREZ CÓRDOBA; SOBRAL, 2017)
Food-packaging	Gallic acid and/or clove oil	Film	Antioxidant and antimicrobial.	(XIONG *et al*., 2021)
Food-packaging	Oregano essential oil	Film	Antibacterial activity.	(HOSSEINI *et al*., 2016)
N/S	*n*-tetradecanol	Microcapsules	Thermal stability, core protection.	(QIN; LI; HU, 2021)
Textile	Rosemary oil	Microcapsules	Antioxidant activity and antibacterial properties.	(SINGH; SHEIKH, 2022)
Tissue engineering	Cinnamon extract	Nanofiber membrane	Degradation, antibacterial activity, and biocompatibility.	(AHMADI *et al*., 2021)
Tissue engineering	Nano-$CaCO_3$	Nanofiber	Thermal stability, antibacterial activity	(TERZIOĞLU, 2021)
Wound dressing	Tannins and platelet-rich plasma	Sponge	Thermostability, mechanical, water absorption	(LU *et al*., 2016)

Ref: Author (2022).

Note: N/S: not specified.

2.4 ENCAPSULATION AND COACERVATION

Encapsulation is a technique by which a polymeric shell can be formed around a liquid droplet or core material acting as a reservoir, with the main aim of protecting the core material from the surrounding environment (ROY *et al*., 2018). This process is made regarding ensure true encapsulation, stability of capsules, prolong storage abilities, suitable release mechanism, and resistance against the harsh environment. Raza *et al*. (2020) summarized the important factors which should be considered in the selection of core and shell materials (Figure 7).

Figure 7 – Important aspects for selection of core and shell materials.

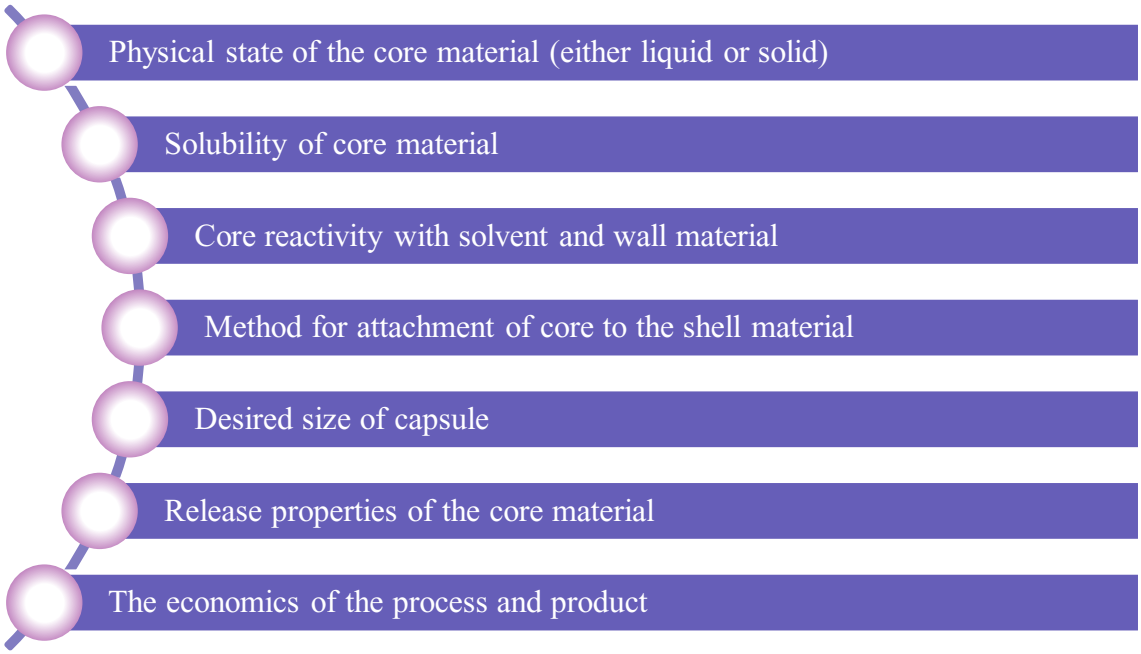

Ref: Adapted from Raza *et al*. (2020).

The formation of capsules can be carried out by various processes such as spray drying, interfacial polycondensation, and complex coacervation (ROY *et al*., 2018). Among them, complex coacervation has received great concern due to its low cost and mild processing temperature; moreover, this method yields spheres with high encapsulation efficiency and anti-oxidative properties, without requiring toxic solvents (MU *et al*., 2022).

Coacervation can be defined as a process in which controlled modification of specific physico-chemical environmental conditions (*e.g.* pH, solubility, ionic strength, temperature) induced phase separation from a liquid medium, leading to a polymer rich phase (the

coacervate) and polymer poor phase (the supernatant) (GONZÁLEZ-MONJE *et al*., 2021; ROY *et al*., 2018). The coacervates phase appears as amorphous liquid droplets, which upon coalescence may separate from the water by gravity (GONZÁLEZ-MONJE *et al*., 2021). This phase separation stage of complex coacervation is known as macro-coacervation (TIMILSENA *et al*., 2017). According to Timilsena *et al*. (2019), the term coacervation was derived from the Latin word *acervus* (meaning "heap") preceded by a suffix "co" indicating an associative phenomenon between two reactants.

The complex coacervation process involves two or more polymers dissolved in the aqueous solution and phase separation occurs by electrostatic interactions, hydrogen bonds, and hydrophobic interactions among the polymer hydrocolloids (ROY *et al*., 2018). Mu *et al*. (2022) explained that the fundamental of complex coacervation is that the core materials are coated by two oppositely charged biopolymers, which can form a complex shell primarily by electrostatic interaction and other driving forces. Li *et al*. (2022) addressed high payload and efficiency of complex coacervation technique, besides high temperature and humidity resistance of the formed microcapsules. Moreover, they highlighted that complex coacervation occurs within a very narrow pH range and stood out the high environmental sensitivity of complex coacervated capsules.

Complex coacervation-based encapsulation process steps were summarized by Timilsena *et al*. (2017). Based in their explanation, a diagram is presented in Figure 8. In the preparation of capsules by the complex coacervation method, a stable emulsion formulation is the crucial step for the final formulation quality, defining the size of the inner single core structures (ROY *et al*., 2017; WANG; ADHIKARI; BARROW, 2014). The next phase is the coacervation step, in which the oil droplets in the emulsion are coated by the coacervates by adjusting the pH of the solution (WANG; ADHIKARI; BARROW, 2014). The complex coacervation process is greatly affected by the properties of the polymers, including their molecular weights, concentrations, and ionic charge densities, which are fixed by the formulations (NAKAGAWA; NAGAO, 2012).

To achieve the desired encapsulation, emulsification and coacervation are followed by deposition of the coacervates on the emulsified droplets in the continuous phase, so the deposited coacervates form a thin layer around the active core material (ROY *et al*., 2018). The coacervates distributes on the interface of colloidal dispersions (*e.g*. oil-in-water emulsion), forming a uniform coating, which jellifies upon cooling, yielding capsules (GONZÁLEZ-MONJE *et al*., 2021). This process can yield single oil droplets covered by an outer shell or

multinucleated capsules. The latter consists of an agglomeration of single cores surrounded by a secondary outer shell, providing a thicker outer shell and improving oxidative stability (WANG; ADHIKARI; BARROW, 2014).

Figure 8 – Complex coacervation-based microencapsulation process steps.

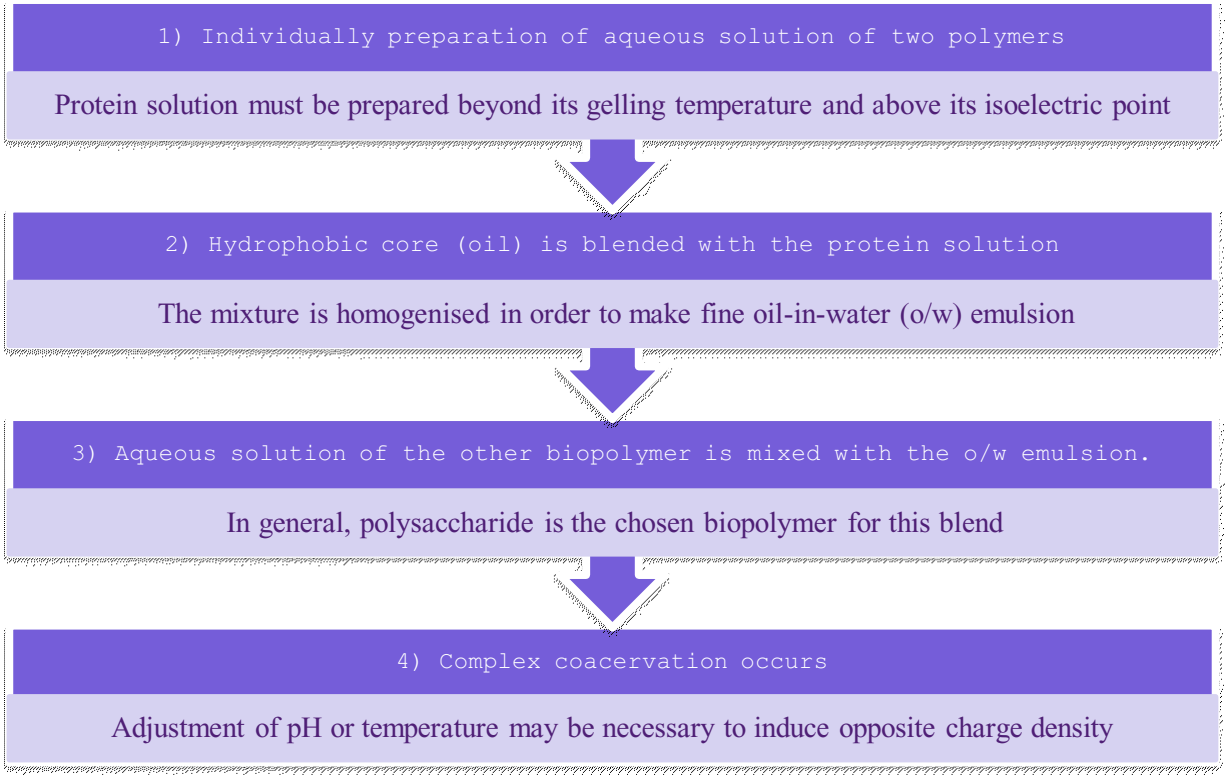

Ref: Author (2022).

Biopolymers may interact with each other through attractive forces in aqueous solutions (MCCLEMENTS; JAFARI, 2018). Electrostatic interaction between chitosan and type B gelatin (GB) for the formation of complex coacervate has been broadly explored in recent years (GONÇALVES *et al*., 2018; PRATA; GROSSO, 2015; VORON'KO *et al*., 2016). Silva and Andrade (2009) evaluated microparticles prepared by complex coacervation at various CS:GB ratios, within the pH range of 3.5 to 6.0 and temperature range of 40 to 60 °C. Results pointed out that the highest yield in microparticles was achieved by using the components with the lowest molar masses, at 60 °C for 4 hours, and chitosan/gelatin ratio of 1:10. Kang, Dai, and Kim (2012) described an emulsification and spray-drying method for the development of microparticles with chitosan and gelatin and pointed out that maximum coacervation between these species occurs at pH 6.0 when the ratio was 1:15, respectively.

Results also demonstrated lower drug releases from microparticles at pH 5.0 and pH 6.0, possibly due to the pH importance in electrostatic interaction between chitosan and gelatin and consequent influence on diffusivity of the drug through the polymer mixture.

Roy *et al*. (2017) studied the behavior of aqueous chitosan, type-B gelatin and CS/GB coacervate on oil-in-water emulsion formulation at various pH and concentration ratios. The authors verified that maximum aggregation of the complexes was observed at pH 5.5, as negative surface charges were developed in aqueous GB (since pH is above its isoelectric point) while CS solutions maintained their cationic nature throughout this pH range. They also stated that electrostatic binding occurred during the formation of complex coacervation at pH 5 - 5.5 and maximum yield of coacervation was observed for 1:10 and 1:5 CS:GB ratio at this pH value.

Another study regarding microencapsulation by complex coacervation of CS:GB biopolymers were developed (ROY *et al*., 2018). High coacervate yield at CS:GB 1:5 and stable emulsion droplets were achieved. Mean diameters decreased upon increasing the homogenization time and size distribution became narrower by increasing GB amount in the biopolymer ratio.

Limonene-containing microparticles were successfully produced by complex coacervation from 10:1 gelatin and chitosan, at 50 °C (PRATA; GROSSO, 2015). It was observed that chitosan, as a large molecule, requires an initial step of unfolding to allow gelatin readily to interact with and encapsulate the active component, and dilute systems were required for this purpose.

Based on the aforementioned data, complex coacervation appears as a promising technique for encapsulation purposes. In this regard, chitosan and gelatin coacervates seem to be an interesting study approach for encapsulation of oil-in-water nanoemulsion.

2.5 COPAIBA OIL

Traditional secular use of copaiba oleoresin to treat wounds was confirmed based on the historic bibliographic research developed by Ricardo *et al.* (2018), and the main applications reported in their ethnobotanical study are pictured in Figure 9 (RICARDO *et al*., 2018). Mentioned in early Portuguese reports in Brazil as a medicine used by native indigenous people, copaiba balsam is still today widely used, especially in regions where the rural population has little access to industrialized pharmaceutical products and conventional health services (CASCON; GILBERT, 2020).

Figure 9 – Traditional uses of copaiba oil.

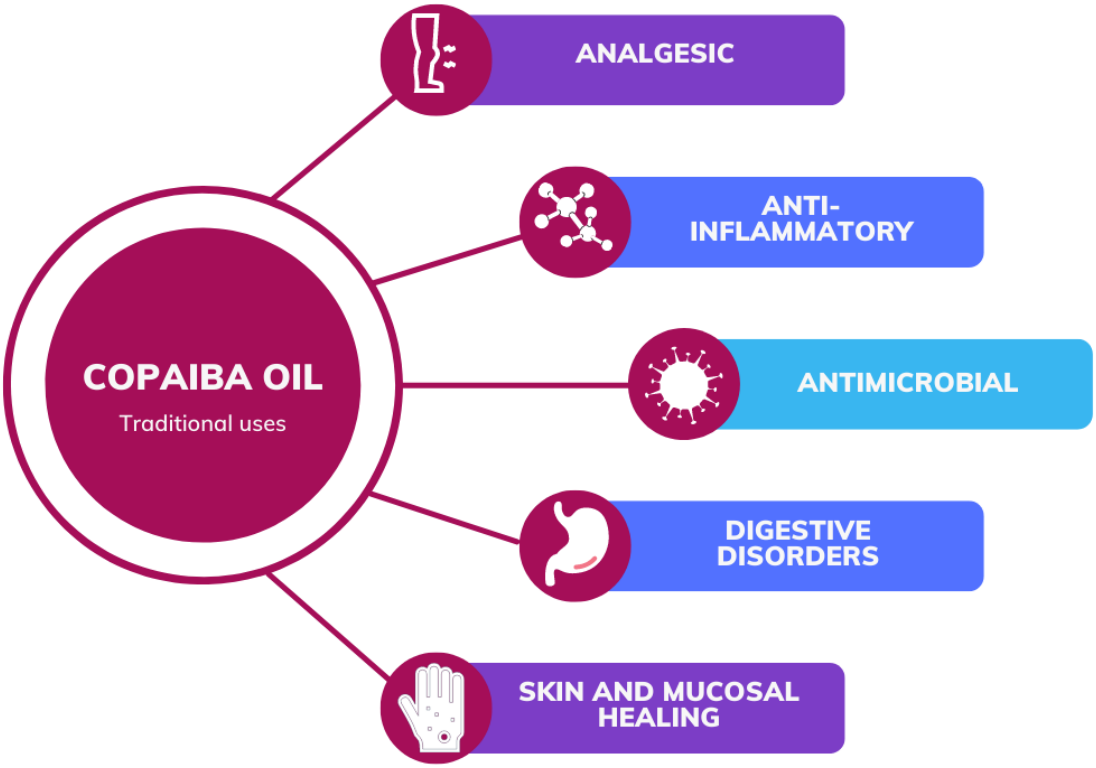

Ref: Author (2022).

Copaiba oil is produced by exudation from the trunks of trees belonging to the genus *Copaifera* (generally *C. reticulata* Ducke species), which is abundant in the Brazilian *flora*, mainly in the amazon rainforest region (ALVARENGA *et al*., 2020; MARANGON *et al*., 2017). It is formed by several components of the bases diterpenes and sesquiterpenes, which concentrations can vary according to species, soil properties, climatic conditions, and the period of the year when the extraction was done (TEIXEIRA *et al*., 2017). Among the main sesquiterpenes found in copaiba oleoresins, β-caryophyllene and its oxide are commonly regarded as the main compounds and responsible for biological activities (antimicrobial and anti-inflammatory) (LEANDRO *et al.*, 2012).

Safety and effectiveness of Copaiba oleoresin on inflammation and tissue repair of oral wounds were assayed by Alvarenga *et al*. (2020). Results demonstrated that systemic administration of the oleoresin promoted an anti-inflammatory effect at an early time point compared to corticoid therapy, accelerating wound resolution. Moreover, biochemical analyses

revealed that the administrated dosage was harmless to the kidneys and liver of rats, endorsing the potential and healing properties of Copaiba oil therapy. Anti-inflammatory and healing capabilities of Copaiba oleoresin-based formulations on the oral cavity were also suggested by Menezes *et al.* (2022) through a systematic review.

Marangon *et al*. (2017) assessed the antimicrobial activity of chitosan/gelatin/copaiba oil emulsions against bacterial strains by minimum inhibitory concentration (MIC) determination. MIC values were defined as the lowest concentrations showing no growth in comparison to the positive control by visual inspection. They evaluated three different copaiba oils and claimed that all of them were able to inhibit *S. aureus* with MIC values ranging from 2.0×10^3 to 62.5 $\mu g.mL^{-1}$. The use of copaiba oil combined with chitosan/gelatin reduced the cytotoxic effect and improved antimicrobial activity, decreasing inhibitory concentrations and response time compared to the isolated compounds.

The effectiveness in reducing chronic inflammatory infiltrate and inhibiting macrophage activity was suggested by Teixeira *et al*. (2017). Biomedical applications were demonstrated by more authors (BONAN *et al*., 2015; DEBONE *et al*., 2019; LIMA *et al*., 2003; VEIGA *et al*., 2007).

Although Copaiba oil has been used orally or topically for many people, it has some drawbacks. For instance, the oxidation of vegetable oils can generate toxic products that can largely affect biological tissues (LAMMARI *et al*., 2021). The water-insoluble nature of copaiba oil may cause an unpleasant feeling when used topically (MARANGON *et al*., 2017). Furthermore, when copaiba oleoresin is used in its natural form for wound healing, it can cause deleterious effects in damaged tissue regeneration, particularly on the re-epithelization step (VIEIRA *et al*., 2008). Beyond that, the volatile character of important copaiba oil components hampers its formulation as a colloidal system (DIAS *et al*., 2014).

To overcome these effects, encapsulation of copaiba oil with biopolymers appears as an interesting perspective, able to overcome some disadvantages and improve oil stabilization. This technique can protect the oil from external factors like oxidation, volatilization, heat, and light (LAMMARI *et al*., 2021). Moreover, it can be a tool for controlling dosage administration that reaches human tissues, apart from enhance healing action. Additionally, for pharmaceutical industry purposes, the production of nanoemulsions of poorly water-soluble compounds improve bioavailability, due to its greater surface area per volume and the extremely low surface tension of the whole system (TANG *et al*., 2012).

2.6 EMULSION

Emulsions are frequently studied as delivery systems of essential oils to achieve uniform distribution of lipophilic compounds in the aqueous phase (XUE; ZHONG, 2014). Basically, an emulsion consists of at least 2 immiscible liquids, usually oil and water, with one of the liquids being dispersed as small spherical droplets in the other. A system that consists of oil droplets dispersed in an aqueous phase is called an oil-in-water (o/w) emulsion (BAKRY *et al*., 2016). Some advantages of these systems are relative ease of preparation, low cost, and aid to sustain the oil or lipid against oxidation and vaporization, among others (ROY *et al*., 2017).

Microcapsules formation and emulsions stability can be enhanced through an appropriate choice of compounds, specially by those who have film form ability and guarantee stability against aggregation; moreover, film forming natural biopolymers such as polysaccharides and proteins have been considered as suitable candidates, thanks to a few other advantages such as non-toxicity, low cost, easy availability, and biocompatibility (ROY *et al*., 2017).

Nanoemulsions can be defined as fine oil droplets (ranging from 100 – 600 nm) dispersed in an external aqueous phase, stabilized by a surfactant system (BOUCHEMAL *et al*., 2004; DIAS *et al*., 2014). It presents a milky aspect, small droplet diameter, and low viscosity, beyond important advantages for biomedical uses, as pictured in Figure 10 (BOUCHEMAL *et al*., 2004; DIAS *et al.*, 2014). Moreover, although nanoemulsions are thermodynamically unstable, they have better physical stability against gravitational separation than conventional emulsions (XUE; ZHONG, 2014).

Figure 10 – Attracting advantages of nanoemulsion for health care applications.

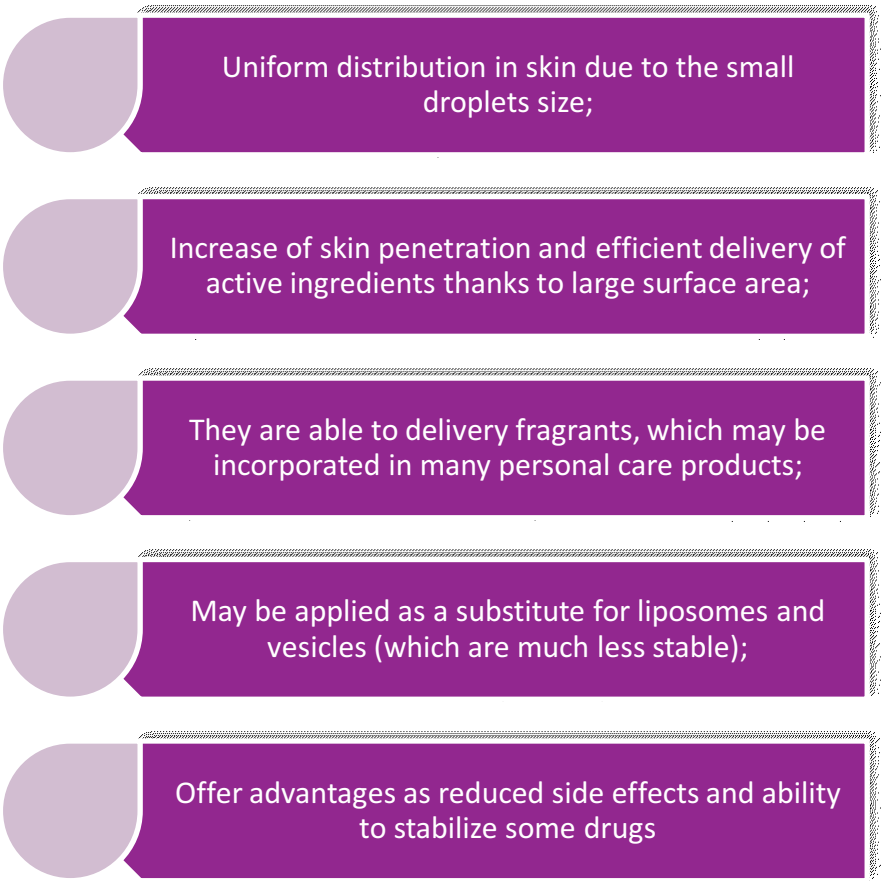

Ref: Author (2022).

The nanotechnology application to prepare pharmaceutical formulations has enabled the incorporation and encapsulation of active substances of interest in nanometric structures, improving efficacy and safety for different treatments (NIGRO *et al*., 2020). In this context, the nanoemulsification of copaiba oil, which has an unctuous character, converts it into a more acceptable hydrophilic formulation and may improve sesquiterpenes penetration through the skin due to the small droplet size and the high contact surface afforded by the nanoemulsions (LUCCA *et al*., 2015).

Emulsifiers are typically amphiphilic molecules that have both hydrophilic and hydrophobic groups on the same molecule, commonly added to the emulsion system in order to obtain a kinetically stable solution (MCCLEMENTS; JAFARI, 2018). Emulsions are prepared by homogenizing both oily and aqueous phases with an emulsifier using a mechanical device (high shear mixer, high-pressure homogenizer, sonicator, among others) (BAKRY *et al*.,

2016). The emulsifier is adsorbed on the interface of oil and water to reduce interfacial tension and keep the droplets stable due to high surface charges; as well its nature also determines the ease of emulsion formation and the functional attributes of the final product. (ROY *et al*., 2017). They are essential to long-term shelf-life and resistance to environmental stresses in nanoemulsion-based products (MARHAMATI; RANJBAR; REZAIE, 2021).

2.6.1 Soy lecithin

Lecithin can be prepared from oil-bearing seeds such as soybeans, sunflower kernels, and rapeseed, and is widely used as a natural emulsifier/surfactant in food, cosmetic, medicine, and biotechnology industries (XUE; ZHONG, 2014). The techno-functional properties of lecithin, as its excellent emulsifying property, are mainly caused by the surface-active character of its predominant polar lipid fraction, the phospholipids (ARNOLD *et al*., 2013).

Soy lecithin (SL) is a mixture comprising 18.0 – 25.0 % phosphatidylcholine, 14.0 – 19.0 % phosphatidylinositol, 10.0 – 16.0 % phosphatidyl ethanolamine, and other chemicals (ZHANG *et al*., 2020a). Phospholipids are a special kind of natural small molecule surfactant that are comprised of a glycerol moiety with a phosphate group and two fatty acid chains (MCCLEMENTS; JAFARI, 2018). Regarded as a low-molecular-weight emulsifier (LMWE), comprised of a hydrophilic head (amphoteric) and a hydrophobic tail, soy lecithin is almost positively charged at acidic pH, neutral at pH 7, and negatively charged at basic pH (ZHANG *et al*., 2020a).

Lecithin-based surfactant mixtures are known for their high biocompatibility, and great emulsifying properties and offer a broad range of applications in pharmaceutical technology (VATER *et al*., 2022). *In vitro* and *in vivo* studies emphasize the skin compatibility of lecithins for the application in skin care products and even indicate a beneficial effect of lecithin treatment on skin health (VATER *et al*., 2019, 2021).

Vater *et al.* (2022) successfully produced oil in water nanoemulsions based on soy lecithin and two lipophilic natural wound healing agents. Their effects on primary human skin cells were studied *in vitro* and results demonstrated that skin cells treated with the loaded formulations had a higher proliferative activity, which is essential for wound closure. Findings suggested that lecithin-based nanoemulsions represent a valid strategy for wound care.

Biopolymer-surfactant interaction could be achieved by different mechanisms (MCCLEMENTS; JAFARI, 2018). Zhang *et al*. (2020b) cited the use of proteins and low-

molecular-weight surfactants together as a way to achieve the physical stabilization of emulsions. Valencia *et al*. (2021) claimed that soy lecithin can improve the properties of the polymeric network formed by opposite-charged biomolecules. They also stated that the rate of incorporation of a bioactive compound is favored by the charged-network and successfully developed soy lecithin/chitosan nanoparticles using the electrostatic self-assembly technique for encapsulation of curcumin. Lopes Rocha Correa *et al*. (2020) produced lecithin-chitosan nanoparticles loaded with melatonin and evaluated its potential for wound healing in diabetic rats. A desired therapeutic effect was achieved through induction of fibroblast, angiogenic proliferation, and expressive collagen deposition.

Gelatin and soy lecithin demonstrated synergistic surface activity to produce translucent and stable thymol nanoemulsions, which greatly enhanced the antimicrobial activity of thymol in different food matrices (LI *et al*., 2020; XUE; DAVIDSON; ZHONG, 2017; XUE; ZHONG, 2014). Zhang *et al*. (2020b) confirmed the synergetic adsorption of gelatin with soybean lecithin in their study, as shown in Figure 11.

Figure 11 – Schematic of synergetic adsorption of G/SL on the oil/water interfaces of oil-loaded emulsions. (A) SL adsorption on the oil/water partial interface of oil droplet. (B) G/SL on the oil/water partial interface of oil droplet.

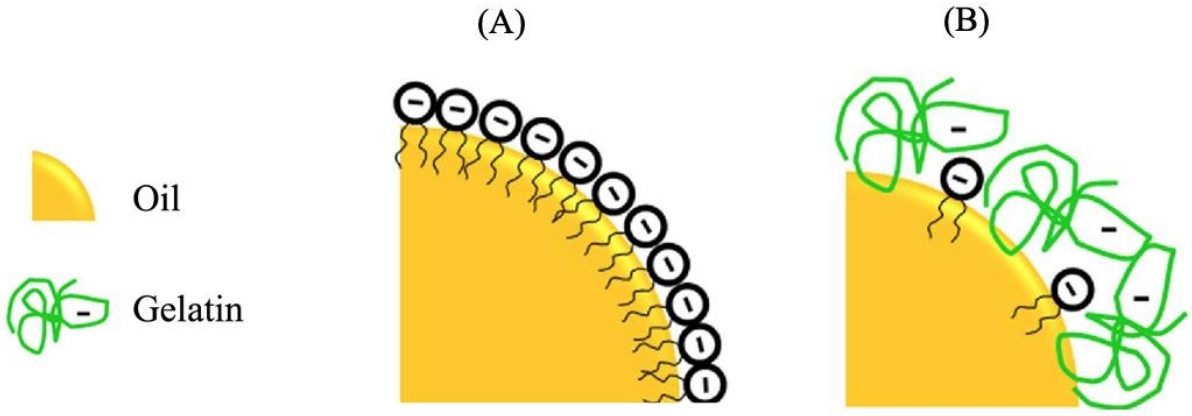

Ref: Adapted from Zhang *et al*. (2020b).

Xue and Zhong (2014) claimed that gelatin and lecithin formed complexes and the mean particle diameter of dispersions with thymol decreased as lecithin concentration increased to about 1% (w/v). The authors explained that beyond that point the radius of droplet curvature reaches a critical value and no further decrease in the particle size is enabled. Their results also

suggest that the more hydrophobic lecithin standing more in contact with the lipophilic drug, while the hydrophilic gelatin binds with lecithin on the particle surface.

Zhang *et al*. (2020b) explored the effects of surfactant type and preparation pH on the fish oil-loaded gelatin/surfactant-stabilized emulsions. Their findings suggest that preparation pH significantly influenced the droplet size of gelatin/soy lecithin stabilized emulsions, which had three types of droplets with different sizes (three peaks). Droplet sizes were significantly linearly decreased with the increase of preparation pH.

Regarding the effect of surfactants on coacervation-based microencapsulation, Mayya, Bhattacharyya, and Argillier (2003) reported an increase in encapsulation yield and propose that encapsulation efficiency is improved by forming a primary layer of surfactant–polyelectrolyte complex over the oil droplets prior to coacervation.

Considering the state of the art, the combination of soy lecithin and gelatin as emulsifiers shows up as an alternative with great potential for the production of oil nanoparticles, aiming for physical stabilization of emulsions with improved bioavailability. Furthermore, due to the excellent bioactivity of chosen compounds, controlled and prolonged delivery of active can enhance therapeutic approaches.

3 MATERIALS AND METHODS

The experimental units used in this work are located in the Laboratory of Process Control and Polymerization (LCP I and IV) of the Department of Chemical Engineering and Food Engineering (EQA) of the Federal University of Santa Catarina (UFSC). However, the characterization equipment is allocated in different research laboratories due to the multidisciplinary nature of the work. Among the partner departments and laboratories are: the Materials Laboratory (LABMAT), the Analysis Center at EQA/UFSC, the Central Electron Microscopy Laboratory (LCME), and the Interdisciplinary Laboratory for the Development of Nanostructures (LINDEN).

3.1 MATERIALS

The reagents used in all preparations and characterizations are of analytical grade, were purchased from commercial sources, and have not undergone prior purification. Type-B gelatin from bovine skin (gel strength 225 bloom), chitosan powder (MM: 190 - 310 kDa, DD 75 - 85%), and glacial acetic acid were obtained from Sigma-Aldrich, Brazil. Copaiba oil and soybean lecithin were purchased from Vita Farma (Floarianópolis, SC, Brazil). Deionized water was used as the solvent. Analytical grade potassium bromide (KBr) pellets were employed for Fourier Transform Infrared (FT-IR) analysis.

3.2 NANOEMULSION SYNTHESIS

For the preparation of the oil-in-water nanoemulsion, (o/w-NE) the experimental route was adapted from Li *et al.* (2020) and Zhang *et al*. (2020b). First, different concentrations, homogenizing speeds (3,400 – 13,000 rpm), and homogenizing times (2 – 30 min) were tested. A series of fourteen experiments were performed in order to build the design of the experimental approach, as shown in Table 2.

The experimental preparation consists of three steps and is illustrated in Figure 12. Briefly, 1% (w/v) gelatin (type B) was dissolved in deionized water (50 mL), at a constant temperature (40 °C) in a water bath for 60 min. The second step consists in the incorporation of 1% (w/v) soy lecithin (surfactant) into the gelatin solution and another 60 min of magnetic stirring, at a constant temperature (40 °C) in a water bath. Copaiba oil (CO) 1% (w/v) was added to the system and the resultant solution was mechanically agitated by an IKA® T25 digital ULTRA-TURRAX® homogenizer, with a homogenizing speed of 13,000 rpm for 360 s.

Figure 12 – Process scheme of nanoemulsion preparation (made with Biorender©).

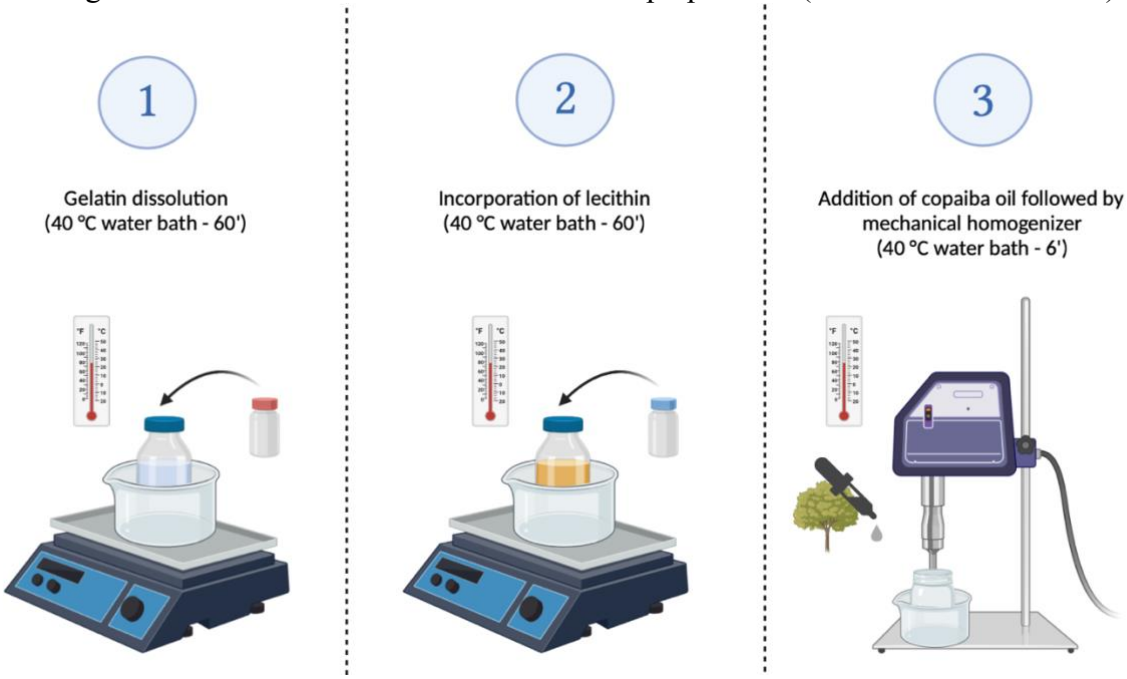

Ref: Author (2022).

Table 2 – Overview of previous settings that were assayed.

Group identification	Gelatin (% w/v)	Surfactant (SL) (% w/v)	Copaiba oil (% w/v)	Homogenizing step	
				(rpm)	Time (min)
T1	4	0.36 (*)	0.5	3,400	6
T2	4	0.5 (*)	0.5	3,400	6
T3	1	0.5	0.5	8,000	2
T4	1	0.5	0.5	8,000	6
T5	1	1	1	8,000	6
T6	1	1	1	11,500	6
T7	1	1	1	13,000	2
T8	1	1	1	13,000	4
T9	1	1	1	13,000	6
T10	1	1	1	13,000	8
T11	1	1	1	13,000	10
T12	1	1	1	13,000	15
T13	1	1	1	13,000	20
T14	1	1	1	13,000	30

Ref: Author (2022).

Note: (*) Dissolved in ethanol under magnetic stirring for 2 h at room temperature before being added to the solubilized gelatin. Adapted from Reyes, Landgraf, and Sobral (2021).

The blending concentration of copaiba oil was selected at 1% (w/v) to get a higher level than the minimum inhibitory concentrations suggested by Marangon *et al*. (2017). Soy lecithin concentration (1% w/v) was defined based on previous studies and test results, which suggest the achievement of smaller particles and narrower distributions of dispersions (LI *et al*., 2020; XIONG *et al*., 2021). The temperature (40 °C, water bath) was controlled during the process. The pH was measured to ensure the range of interest.

3.3 COACERVATION PROCESS

Three different concentrations of chitosan were prepared for coacervation process evaluation, as presented in Table 3. Chitosan was dispersed in an aqueous solution (10 mL) of glacial acetic acid (0.3% v/v) under magnetic stirring at room temperature for 24 h to completely solubilize. As the concentration of gelatin for preparation of o/w-NE was fixed at 1% (w/v), CS concentration changed accordingly at various weight ratios of 1:15, 1:10, and 1:5.

Table 3 – Experimental groups for coacervation tests.

Group identification (*)	**Chitosan Concentration (g/10 mL)**	**Weight ratio CS:G**
1:15 CS:G	0.03	1:15
1:10 CS:G	0.05	1:10
1:5 CS:G	0.1	1:5

Ref: Author (2022).

Note: (*) Group identification is related to the CS:G weight ratios and the concentration of gelatin remain constant (0.5 g/ 50 mL) for all tests.

These chitosan concentrations were selected based on previous studies, which demonstrated highest encapsulation yield through complex coacervation with gelatin (PRATA; GROSSO, 2015; ROY *et al*., 2017, 2018; SILVA; ANDRADE, 2009). To prepare coacervate particles, the corresponded CS solution was mixed dropwise with copaiba oil nanoemulsion (described in 3.2) and stirred for 4 h, 200 rpm, at 40 °C, as pictured in Figure 13.

The pH of the mixture was measured to certify that it was higher than gelatin Ip. The selected pH for the coacervation process was 5.0. Once the coacervation took place, the system was brought to room temperature (approximately 20 °C) to harden the microcapsules for 24 h, as illustrated in Figure 14.

Figure 13 – Magnetic stirring of CS and o/w-NE to prepare coacervate microparticles.

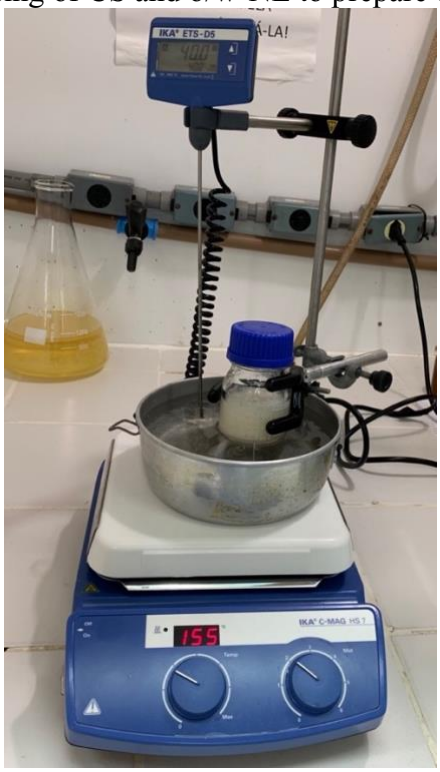

Ref: Author (2022).

Figure 14 – 1:10 CS:G coacervate after 24 h at room temperature.

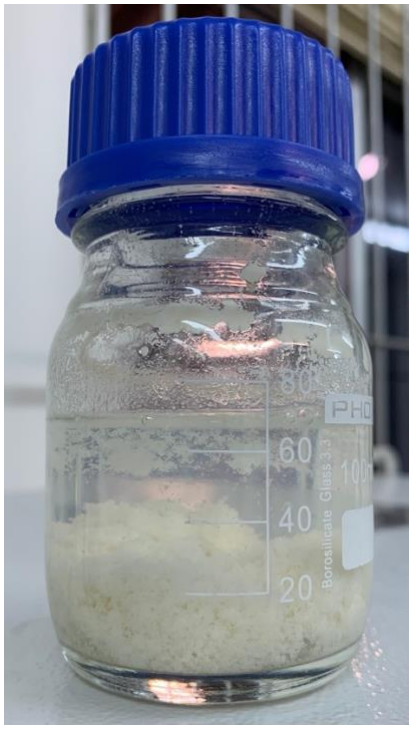

Ref: Author (2022).

3.4 PRELIMINARY CHARACTERIZATION

3.4.1 Gas chromatography/mass spectrometry analysis

Considering that copaiba oil is obtained from trees of the *Copaifera* genus, and for that reason, its chemical composition can vary according to different raw sources (*e.g.* species, soils, and time of the year). In this regard, the GC/MS of copaiba oil utilized in this dissertation was analyzed in order to properly characterize this material. The GC/MS analysis was performed on instrument Agilent GC 7890A coupled with MS detector Agilent 5975C. The column, a HP-5MS (Agilent) fused silica capillary column (30 m length x 250 µm i.d. x 0.25 µm film thickness composed of 5% phenyl-95% methylpolysiloxane) was connected to a EI source **(**Electron Impact Ionization) operating at 70 eV with a quadrupole mass analyser. The mass scan ranged from 41 to 415 m/z. Helium was used as the carrier gas at a flow rate of 1.0 mL min^{-1}. The injector (with a split ratio of 1:20) and interface temperatures were at 220 ºC and 240 ºC, respectively. The solvent delay was 3.0 minutes. The injection volume was 0.2 µL with auto sampler Agilent GC Sampler 80 equipped with a 10 µL syringe. The oven temperature program consisted of ramping up from 60 ºC (3 °C/min) to 246 °C (total run time of 62 min). The compounds were identified by comparing their mass spectra with those from the National Institute of Standards and Technology (NIST, 2011). Linear Retention indexes were calculated by the retention times of n-alkanes that were injected under the same chromatographic conditions (ADAMS, 2007; BIZZO *et al*., 2020).

3.4.2 Evaluation of free surface charge

The determination of the variation of Zeta potential (Zp) of individual polymers with pH was made to correct elucidate the coacervation process, mainly because allows the selection of the optimum pH at which complex coacervation occurs (TIMILSENA *et al*., 2019; WANG; ADHIKARI; BARROW, 2014). For that reason, the Zeta potential values of gelatin and chitosan within a pH range of 4.0 - 6.0 were analyzed.

Gelatin solution (0.1% w/v) was prepared by dissolving the precursor protein directly in distilled water and further stirring for at least 12 hours at 45 °C. Analogously, chitosan solution (0.1% w/v) was prepared by the same method (LI *et al*., 2022a). Hydrochloric acid and sodium hydroxide was employed to adjust the pH to a desirable range. The Zp values of the

solutions were determined at 25 °C using a Zetasizer Nano-ZS (Malvern Instruments, LINDEN, UFSC) capable of electrophoresis measurements.

3.5 NANOEMULSION CHARACTERIZATION

3.5.1 Droplet size, Zeta-potential, and polydispersity index (PdI)

The aim of the test was to investigate the stirring variables (speed and time) for achieving uniform and small droplets of an oil-in-water nanoemulsion (o/w-NE). The hydrodynamic diameter of the copaiba oil droplets was determined by dynamic light scattering (DLS) using a Zetasizer Nano-S (Malvern Instruments Ltd, Laboratory of Process Control and Polymerization, UFSC), at 25 °C, using a transparent glass cuvette. The scattered angle was fixed at 173° and no sample dilution was necessary. Results were presented as the average of three runs, expressed as the intensity average diameter and the polydispersity index (PdI). The PdI is a dimensionless measure of the width of size distribution calculated from the cumulant analysis ranging from 0 to 1 (TANG *et al*., 2012). Lower PdI values correspond to a more monodispersed population, while a large PdI indicates a broader distribution of droplet size Tukey's mean separation test was applied as statistical analysis for the average mean particle diameters comparison. The Zeta potential of the o/w-NE was measured using a Zetasizer Nano-ZS (Malvern Instruments, LINDEN, UFSC), at 25 °C.

3.6 COACERVATED CHARACTERIZATION

3.6.1 Fourier-transform infrared spectroscopy (FT-IR)

Fourier Transformed Infrared spectrometer (AGILENT TECHNOLOGIES – Cary 660 FTIR, Brazil) was applied to identify the structures of the coacervates and raw materials applied in the process. The data were collected in the range of 400 – 4000 cm^{-1} at a 4 cm^{-1} resolution, and the total scan times were 32. The infrared spectrum of pure KBr was selected as a baseline.

3.6.2 Optical microscopy (OM)

For morphological analysis, digital images of coacervate particles were collected through the Leica DM4000 M optical microscope and Leica DFC450 camera. The coacervate

samples were deposited on the glass substrate. Adapted from (GONZÁLEZ-MONJE *et al.*, 2021).

3.6.3 Coacervation yield (CY)

To investigate which CS:G ratio provided maximum coacervate outcome at defined experimental conditions, processes yield was assessed. After coacervation, the majority of the precipitated particles were separated using vacuum filtration with filter paper (Unifil 501.1260 – mesh 4-12 Âμm) and weighed. Samples were dried at 60°C until the weight remained constant. Considering the significant losses of coacervated materials that stuck at instruments applied for this technique, as demonstrate in Figure 15, the vessel used for the coacervation process was also weighed and dried at 60°C until the weight remained constant.

The yield of the process was calculated as the percent of dry material precipitated in relation to the initial dry mass (mass of polymers on a dry basis) – Equation (1). Adapted from (PRATA; GROSSO, 2015) and (WANG; ADHIKARI; BARROW, 2014).

$$CY = \frac{m_i}{m_0} \times 100 \quad (1)$$

where CY is the coacervates yield (%), m_i is the mass values (g) of dried coacervates and m_0 is the total mass of both gelatin, chitosan, soy lecithin, and copaiba oil. Adapted from (WANG; ADHIKARI; BARROW, 2014).

Figure 15 – Coacervate accumulation in Pasteur pipettes utilized in this procedure.

Ref: Author (2022).

3.6.4 Transmission electron microscopy (TEM)

Particle morphology was observed by Transmission Electron Microscopy using a JEM-2100F (100Kv). The sample, obtained from group 1:5 CS:G, was diluted in distilled water and dispersed in an ultrasound bath for 60 min. One single drop was placed on a carbon-coated copper grid. The samples were analyzed after drying for 48 h at room temperature. Observations were carried out in the Central Electron Microscopy Laboratory (LCME) of the Federal University of Santa Catarina.

4 RESULTS AND DISCUSSION

In this chapter, the experimental results obtained in the development of this dissertation are presented. In Section 4.1 and 4.2, the characterization of copaiba oil and Zeta potential measurements for complex coacervation are discussed. Section 4.3 addresses nanoemulsion characterization. Sections 4.4, 4.5, 4.6, 4.7, and 4.8 present the coacervated characterization results obtained with optimized o/w-NE conditions.

4.1 COPAIBA OIL GAS CHROMATOGRAPHY (GC) ANALYSIS

The chromatogram profile and chemical composition of Copaiba oil used in the experiments conducted in this dissertation are shown in Figure 16 and Table 4, respectively.

Figure 16 – Chromatogram profile of Copaiba oil.

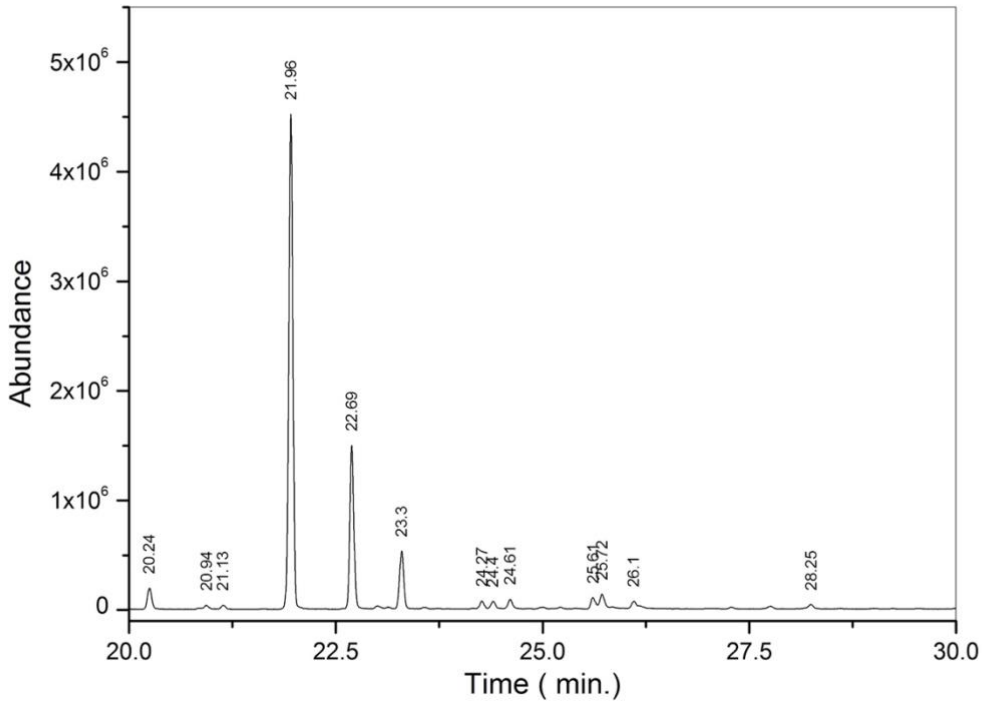

Ref: Author (2022).

The predominant sesquiterpenes detected were β-Caryophyllene, *trans*-α-Bergamotene, α-Humulene, and α-Copaene, components that are commonly found in copaiba oleoresins as in several essential oils (LEANDRO *et al*., 2012). These substances were

identified by computerized matching and comparison of the spectra obtained with those from the databank, considering the linear retention index (LRI), as described in the Experimental section (ADAMS, 2007).

Copaiba oil is known as the major natural source of β-Caryophyllene, which is regarded as a bactericidal, anti-inflammatory compound, and possess the ability to treat chronic pain (DIAS *et al*., 2014; LUCCA *et al*., 2015; PARISOTTO-PETERLE *et al*., 2020). Cascon and Gilbert (2000) stated that caryophyllene oxide is a genuine product of the secondary metabolism of *Copaifera* and discarded previous interpretation in which this component was regarded as an oxidative artefact produced during storage of copaiba oil.

Chronic inflammatory states of the intestines and associated symptoms (such as diarrhea and tissue disruptions) have been treated with *trans*-α-Bergamotene in folk medicine, and its combination with β-bisabolene (an anti-inflammatory compound) seems to perform a good activity against oral pathogens (BONAN *et al*., 2015; ORF *et al*., 2018). The α-Humulene has been related to the promotion of angiogenesis, helpful in wound healing, and anti-inflammatory response (ALVARENGA *et al*., 2020). Antitumoral activity has been attributed to α-humulene, β-caryophyllene, and α-copaene, due to their cytotoxic potential and ability to inhibit the growth of cancer cells (MENDES DE LACERDA LEITE *et al*., 2021). A significant antifungal potential is also attributed to α-copaene (MENDES DE LACERDA LEITE *et al*., 2021). The chemical composition of Copaiba oil are presented in Table 4.

Table 4 – Chemical composition of CO used in this dissertation determined by GC/MS.

Identified component	**Retention Time (min)**	**% GC/MS**
α-Copaene	20.25	2.64
β-Elemene	20.94	0.47
β-Caryophyllene	21.96	59.20
Trans-α-Bergamotene	22.70	19.44
Cis-β-Farnesene	23.01	0.49
α-Humulene	23.30	6.95
γ-Muurolene	24.27	0.88
Germacrene D	24.40	0.89
α-Muurolene	25.22	0.20
β-Bisabolene	25.61	1.51
Butylated Hydroxytoluene	25.72	2.10
γ-Cadinene	26.10	1.06
Caryophyllene oxide	28.25	0.56

Ref: Author (2022).

The results obtained are in agreement with the literature, *i.e.*, many studies have shown sesquiterpenes and diterpenes as the main compounds found in copaiba oleoresins; however, environmental factors and differences between species influence its composition and biological activity (MARANGON *et al.*, 2017).

4.2 OPTIMUM PH FOR COMPLEX COACERVATION

One methodology widely used in the selection of optimal processing conditions for encapsulation by complex coacervation is the determination of available charges of polymers involved in the process (PRATA; GROSSO, 2015). The electrostatic interaction between the two oppositely charged macromolecules contributes to the major driving force, which is highly dependent on the pH (MU *et al.*, 2022). As explained (TIMILSENA *et al.*, 2017), the most favorable complexation is usually observed at a pH value where the charge difference between participating polymers is at maximum value.

In this dissertation, type B gelatin was applied for o/w-NE development and expected to act both as shell material for oil droplets and to react with chitosan in the second stage of the

complex coacervation process. Therefore, the distribution of charges for the chosen protein was measured by Zeta potential, as presented in Figure 17, regarding identify the range of probability for interaction with chitosan.

Figure 17 – Zeta potential measurements of gelatin as a function of pH for coacervation assessment.

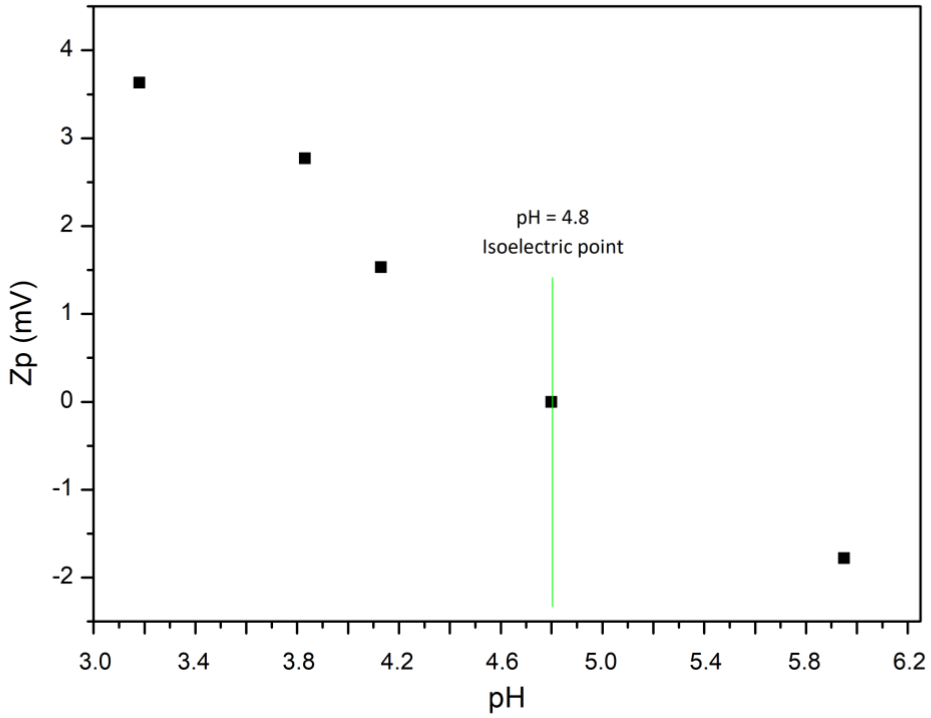

Ref: Author (2022).

As shown in Figure 17, the gelatin isoelectric point was at pH 4.8, where above that point this biopolymer became negatively charged due to the losing H^+ from anionic COOH groups (PRATA; GROSSO, 2015; ROY *et al*., 2017). Considering that the interaction occurs mainly due to electrostatic forces between oppositely charged polymers (GONÇALVES *et al*., 2018), measurements below this point were dismissed for further analysis. Furthermore, chitosan has a limited application window mainly because it is insoluble at pH values higher than 6.5 (GONÇALVES *et al*., 2018). The establishment of this scope is the first guideline for the obtention of particles with this pair of polymers (PRATA; GROSSO, 2015). In this regard, the Zp of chitosan for the selected pH range is shown in Table 5.

Table 5 – Zeta potential measurements of chitosan as a function of pH for coacervation assessment.

	Measurements			
pH	4.76	5.03	5.08	6.16
Zeta potential (mV)	51.4	53.8	48.9	48.5

Ref: Author (2022).

From Table 5 it is concluded that chitosan is completely presented in the cationic form for the tested pH range and reached a maximum value at pH 5.03 (53.8 mV). In view of the slight difference found in gelatin surface charges for pH higher than Ip, a comparable charge magnitude between Zp results obtained for both biopolymers applied in this study indicate that pH 5 is the optimum point for complex coacervation. This finding agrees with other studies (LI *et al*., 2022b; WANG; WANG; HEUZEY, 2016).

It is important to highlight that more tests should be performed to obtain the Zeta potential of chitosan in the pH range between 5.03 and 6.16 for a complete assessment of charges, since their electrostatic interaction could be employed to indicate their binding strength for coacervation (HONG; MCCLEMENTS, 2007; WANG; ADHIKARI; BARROW, 2014).

4.3 DROPLET SIZE, ZETA-POTENTIAL, AND POLYDISPERSITY INDEX

The copaiba oil nanoemulsion was carried out in the presence of gelatin and soy lecithin assuming that their combined use would provide physical stabilization of emulsions and enhance the bioactivity of the resultant nanospecies. All prepared formulations were analyzed by dynamic light scattering (DLS). However, it was not possible to form stable nanoemulsions with all tested experimental conditions, and therefore these formulations were excluded from further investigations. Mean droplet size and PdI results are presented in Table 6.

All tests resulted in solutions with a milky white aspect, because of the distribution of gelatin in the solution (DING *et al*., 2020). As presented in Table 6, tests performed at 3,400 rpm made particles detection unfeasible, probably due to the high diameter of the particles. This can be associated to the homogenizing step, which was insufficient for adequate droplet breaking and dispersing.

Size distributions depended on the applied homogenizing time when the speed rate went up to 8,000 rpm. For groups T3 and T4 (both containing 0.5% w/v SL and 0.5% w/v CO),

an homogenization time increase of 4 min evidenced an outset of PdI refinement. When surfactant and oil concentrations were raised for 1% w/v each, group T5, and the homogenizing parameters were preserved, great progress was achieved: nanoparticles diameters and PdI decreased significantly.

Table 6 – Droplet size and PdI of tested groups.

Group identification	**Homogenization step**		**Mean droplet size (nm) (± SD)**	**PdI (± SD)**
	(rpm)	**Time (min)**		
T1	3,400	6	NPD	-
T2	3,400	6	NPD	-
T3	8,000	2	756 ± 22.72	1.000 (*)
T4	8,000	6	869 ± 12.99	0.607 ± 0.008 (**)
T5	8,000	6	370 ± 4.869	0.369 ± 0.064 (**)
T6	11,500	6	281.3 ± 4.557	0.317 ± 0.010
T7	13,000	2	292.7 ± 6.307	0.288 ± 0.011
T8	13,000	4	299.3 ± 5.541	0.306 ± 0.005
T9	13,000	6	281.6 ± 5.813	0.293 ± 0.006
T10	13,000	8	300.4 ± 6.879	0.335 ± 0.041
T11	13,000	10	331.3 ± 3.808	0.405 ± 0.048
T12	13,000	15	288.5 ± 1.803	0.328 ± 0.047
T13	13,000	20	319.3 ± 6.338	0.331 ± 0.009 (**)
T14	13,000	30	298.3 ± 6.351	0.323 ± 0.009 (**)

Ref: Author (2022).

Notes: NPD: no particles detected.
(*) Contains large particles/aggregates. Sample too polydisperse for cumulant analysis.
(**) Sample too polydisperse for cumulant analysis.

This result presents the importance of surfactant concentration. A correspondent effect was also observed by Xue and Zhong (2014) when preparing thymol nanodispersions with gelatin and soy lecithin. Authors claimed that a greater amount of SL enables the stabilization of a larger interfacial area, leading to smaller particles until reaching a critical value beyond

which no further decrease in the particle size is enabled. Their findings indicated that this critical point was reached with 1% (w/v) of SL.

Results obtained when the homogenizing speed reached 11,500 rpm, group T6, demonstrated an evidential reduction in the nanoparticle diameter size, although just a slight improvement was achieved for PdI values. As homogenization parameters are commonly highlighted as significant variables for tuning the narrow size distribution and influence particle diameter, a higher speed was evaluated.

Roy *et al*. (2017) described a strong dependence between increased homogenization time and shrinkage of emulsion droplet mean diameter. They concluded that optimized results were achieved after homogenization at 13,500 rpm for 30 min. In this regard, groups T7 until T14 were planned for process time assessment. The relationship between tested stirring speeds (from 11,500 until 13,000 rpm) and the mean diameter obtained was shown in Figure 18.

Figure 18 – Mean particles diameters comparison for different groups.

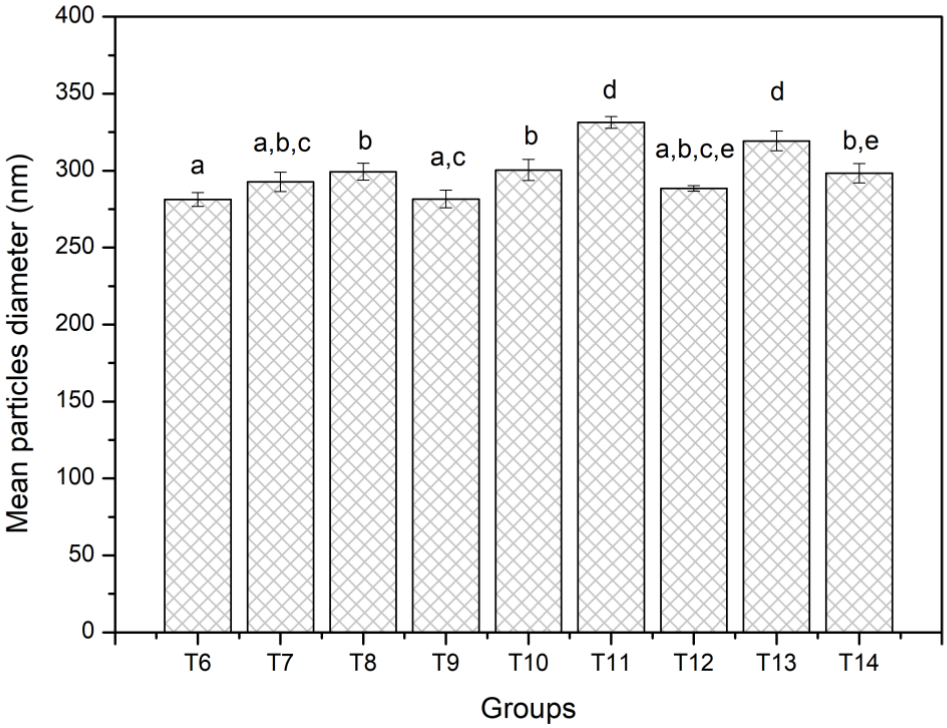

Ref: Author (2022).

Notes: Groups with different letters (a,b,c,d,e) are significantly different ($p < 0.05$) for Tukey's mean separation test.

The emulsions mainly consisted of droplets with a trimodal size distribution, with the mean diameter ranging from 281.3 nm to 331.3 nm with PdI values from 0.288 to 0.405. Even though the droplet sizes were statistically different, PdI values remained below 0.6, given indictments of droplets homogeneity in the formulations (NORCINO *et al*., 2020).

Droplet sizes of gelatin-stabilized emulsions are expected to decrease linearly with increasing homogenizing time, and decrease exponentially with increasing homogenizing speed (DING *et al*., 2020; ZHANG *et al*., 2020d). However, an opposite and significant effect on droplet size was observed when increasing the homogenizing time over 10 minutes, which was probably related to the fast adsorption of soy lecithin on the oil droplet (LI *et al*., 2020).

LMWEs, such as soy lecithin, are associated with faster adsorption at the interface of o/w, which decreases the interfacial tension and particle size; moreover, they are absorbed more rapidly at the particle surface than biopolymers (MARHAMATI; RANJBAR; REZAIE, 2021). Additionally, over processing is known for influence the formation of particles of larger size (YONG; ISLAM; HASAN, 2017).

The droplet size of the nanoemulsion is of highest importance for the dissolution rate of drugs with low water solubility, as can determine the pharmacokinetic and biodistribution pattern of the compound upon systemic administration (TANG *et al*., 2012). Therefore, group T9 (13,000 rpm for 6 min) was chosen for further tests, as presented the most improved results for mean particle diameter (281.6 ± 5.813) and lower PdI values (0.293 ± 0.006) when compared with other groups. Moreover, size distribution showed an excellent similarity pattern for different samples, as can be seen in Figure 19.

Another parameter used to predict the stability of colloidal emulsions is the Zeta potential, as it reflects the surface potential of the particles (VALENCIA *et al*., 2021). The Zp is a measure of how strongly the droplets of a nanoemulsion repel each other to prevent coalescence from occurring, keeping them stable (NORCINO *et al*., 2020).

The Zeta potential of o/w-NE obtained under the optimizing experimental conditions (group T9) was -13.067 mV. The negative value suggests that gelatin was covering the nanoemulsion surface as expected.

At the pH close to the isoelectric point, proteins are expected to have a low negative charge (MARHAMATI; RANJBAR; REZAIE, 2021). Considering that the pH during o/w-NE preparation was 5.9, this result is consistent with the literature.

Figure 19 – Droplet size distribution of o/w-NE (T9). Each line represents one result obtained from test performed in triplicate.

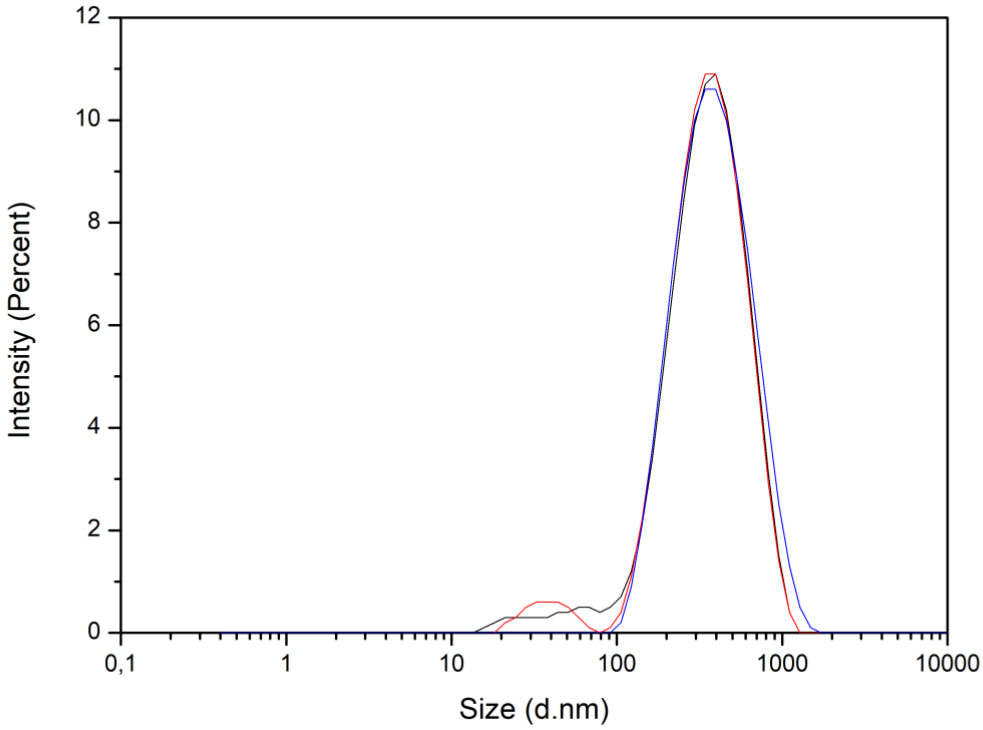

Ref: Author (2022).

4.4 FT-IR

To confirm the formation of complex coacervates and the efficiency of this method for encapsulation of copaiba oil, FT-IR spectrum of the coacervate and the isolated materials were taken and shown in Figure 20. The infrared spectra of copaiba oil showed characteristic bands, highlighting the region between 2925 cm^{-1} and 2854 cm^{-1}, attributed to the C–H bonding axial deformations in aliphatic hydrocarbons, such as sesquiterpenes and other organic compounds found in this oil (FERREIRA *et al.*, 2014; NORCINO *et al.*, 2020). The band at 3008 cm^{-1} is attributed to the C–H stretching of alkenes. Bands at 1461 cm^{-1} and 1376 cm^{-1} are referred to the axial strains of C–H bonds (NORCINO *et al.*, 2020).

The FT-IR spectrum of soy lecithin showed peaks at 1741 cm^{-1}, 1463 cm^{-1}, and 1070 cm^{-1}, assigned to carbonyl stretch, C–H bending vibrations of the alkanes, and presence of

phospholipids, respectively (SHAH; GAITONDE; GANESH, 2018). The absorption peak at 2925 cm^{-1} was due to C–H stretching of the CH_3 groups, present in soy lecithin and copaiba oil (SINGH *et al*., 2016). The peak at 3010 cm^{-1} is assigned to the C–H stretching of alkenes.

The spectrum of gelatin showed a peak at 3436 cm^{-1}, attributed to O–H stretching (XU *et al*., 2020). Moreover, three major bands at approximately 2925 cm^{-1}, 1639 cm^{-1}, and 1556 cm^{-1} were assigned to amide B (antisymmetric and symmetric stretching of C–H), amide I (C=O stretching), and amide II (N–H bending and C–N stretching vibrations) bands, respectively (CEBI *et al*., 2016; XU *et al*., 2020).

Chitosan shows a broad band ranging between 3600 and 3000 cm^{-1}, attributed to the O–H and N–H stretching vibration, and a broad band between 3000 and 2800 cm^{-1}, which represents the C–H stretching vibration (FERREIRA *et al*., 2014; JRIDI *et al*., 2014; PELISSARI *et al*., 2009). The peaks observed at 1658, 1592, and 1421 cm^{-1} are assigned to amide I, amide II, and amide III, respectively (CHEN *et al*., 2016).

Regarding the spectrum of the coacervate, the band at 3008 cm^{-1}, which is attributed to the C–H stretching of alkenes, indicates copaiba oil presence in the compound. Another suggestion that the coacervate retained the oil is the increase in the intensity of the bands 2927 cm^{-1} and 2854 cm^{-1} (sesquiterpenes), which differ from the original spectra of each biopolymer (NORCINO *et al*., 2020). Shifts in peak 1743 cm^{-1} and a higher intensity of the peak at 2854 cm^{-1} were highlighted by more authors to confirm the incorporation of oils into the polymer matrix containing chitosan (FERREIRA *et al*., 2014; HOSSEINI *et al*., 2016; PÉREZ CÓRDOBA; SOBRAL, 2017).

The addition of chitosan in gelatin caused conformational changes, such as peaks of chitosan at 3010 and 1037 cm^{-1} shifting to 3008 and 1095 cm^{-1}, respectively, due to electrostatic interactions for the amino and carbonyl groups (LI *et al*., 2022a; XU *et al*., 2020). The shifting revealed that chitosan was coated on o/w-NE by an electrostatic attraction.

Moreover, when chitosan was applied for complex coacervation, the amide-II (1592 cm^{-1}) peak shifted to 1542 cm^{-1}, which suggested that there was a hydrogen bonding interaction between chitosan and o/w-NE (LI *et al*., 2022a; PELISSARI *et al*., 2009; XU *et al*., 2020). The analysis of FT-IR spectra allowed confirming the oil incorporation on the coacervate.

Figure 20 – FTIR spectrum of coacervate and blank samples.

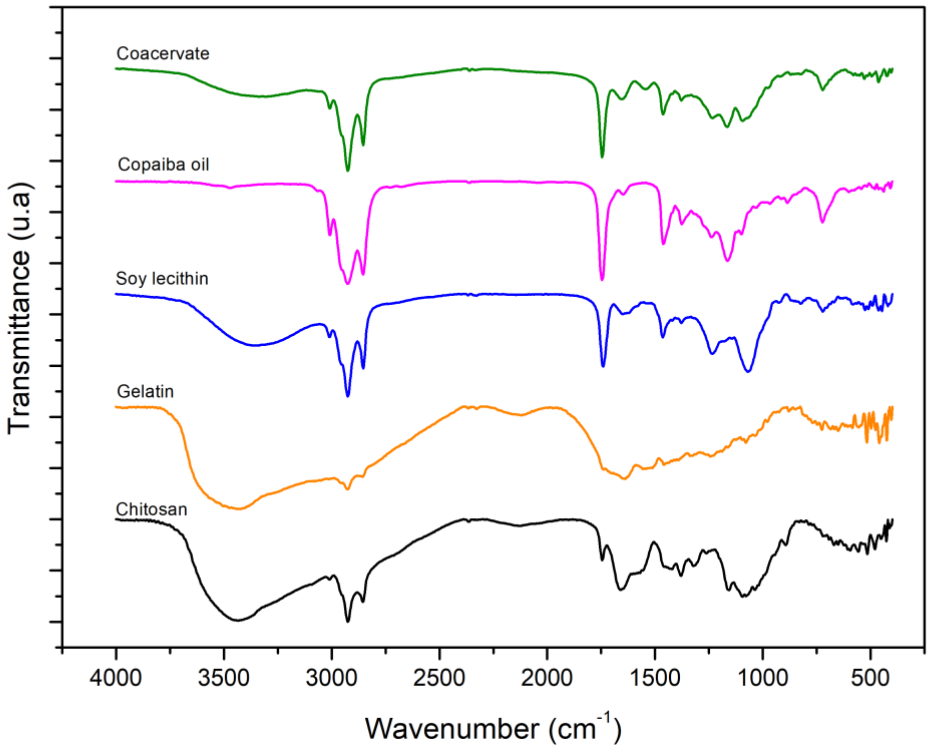

Ref: Author (2022).

4.5 MORPHOLOGICAL ANALYSIS

Optical microscopy was used to study the morphology of the complexes formed with gelatin molecules present at the outer layer of o/w-NE and different proportions of chitosan, managed at pH 5. As previously mentioned, nanoparticles with less than 300 nm containing copaiba oil as core material were created from the nanoemulsion process.

Electrostatic attraction between oppositely charged groups of chitosan and gelatin at the settled process pH was expected to lead the formation of complex coacervates (MCCLEMENTS; JAFARI, 2018). Figure 21 presents the obtained images for each group.

Optical microscopy images evidence encapsulation by chitosan, once identification of beads was possible. Although frequency distribution study of droplet sizes was not possible in this equipment, spherical shapes appear as a signal of oil droplets inside the aggregates.

Figure 21 – Images obtained from optical microscopy: (A and B) Group 1:15 CS:G; (C and D) Group 1:10 CS:G; (E and F) Group 1:5 CS:G. All images were captured with a magnification of 400x. Scale bars indicate 50 µm.

(A)

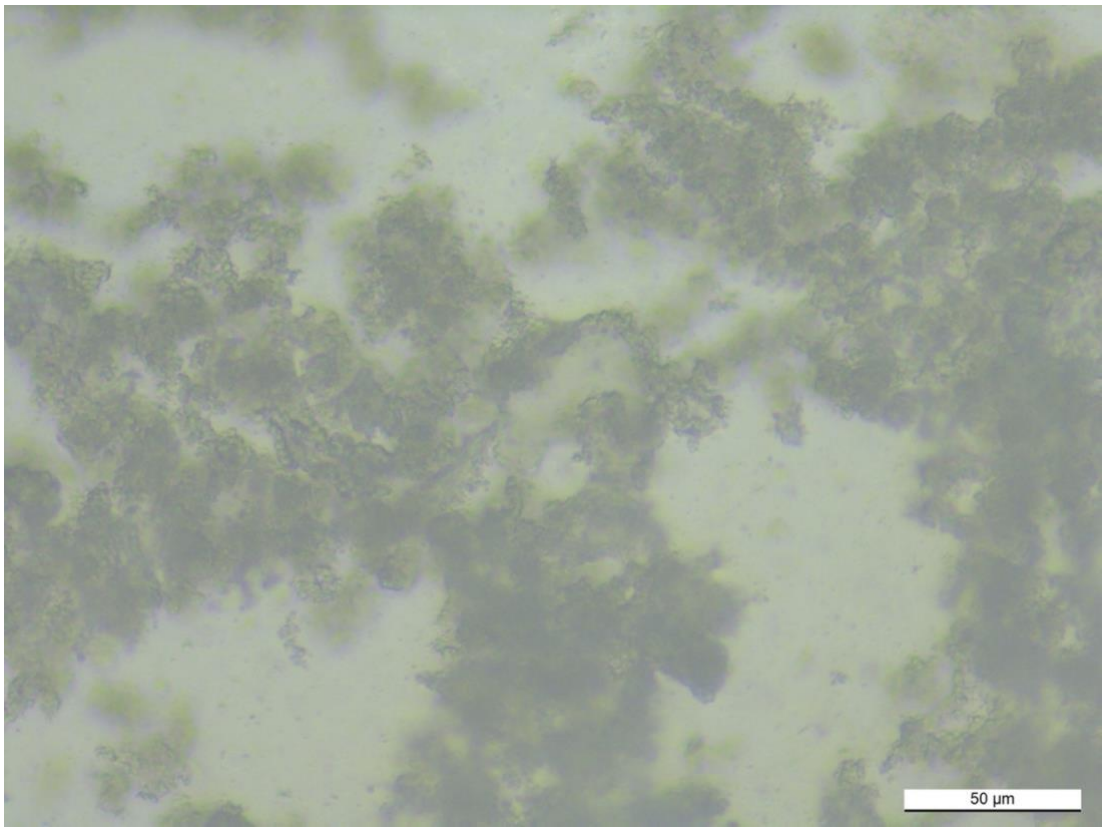

(B)

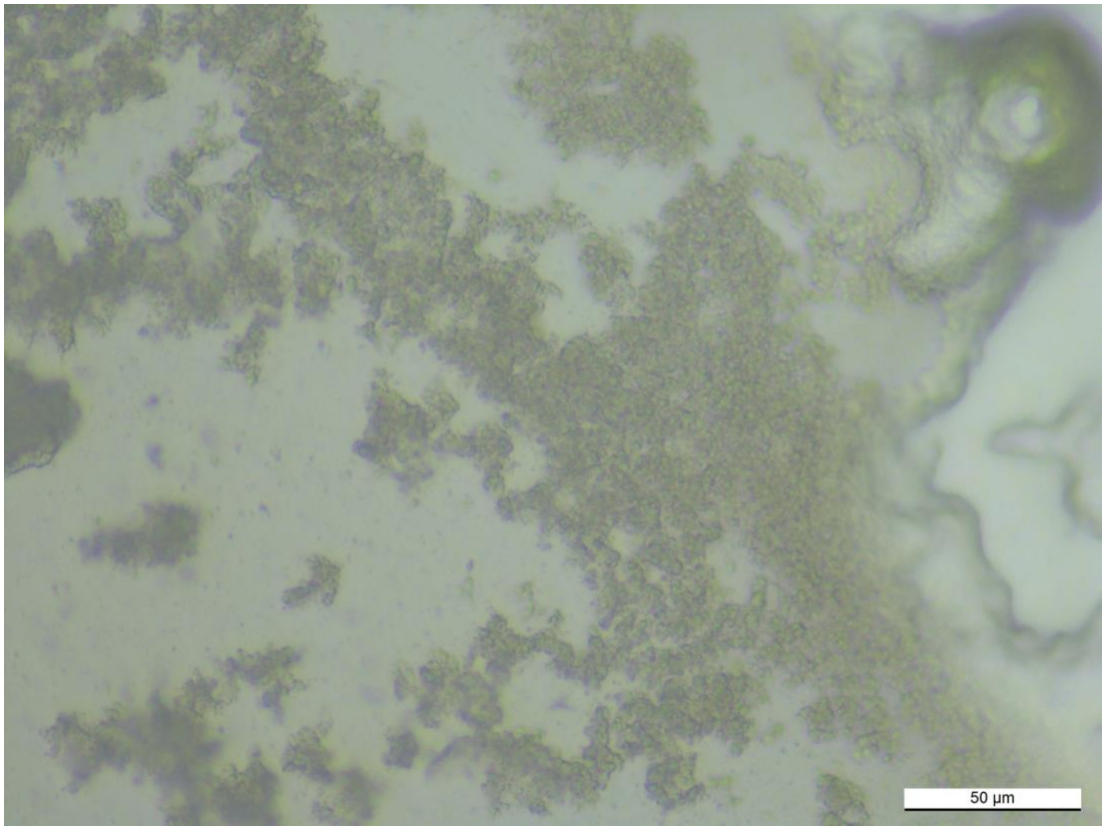

(C)

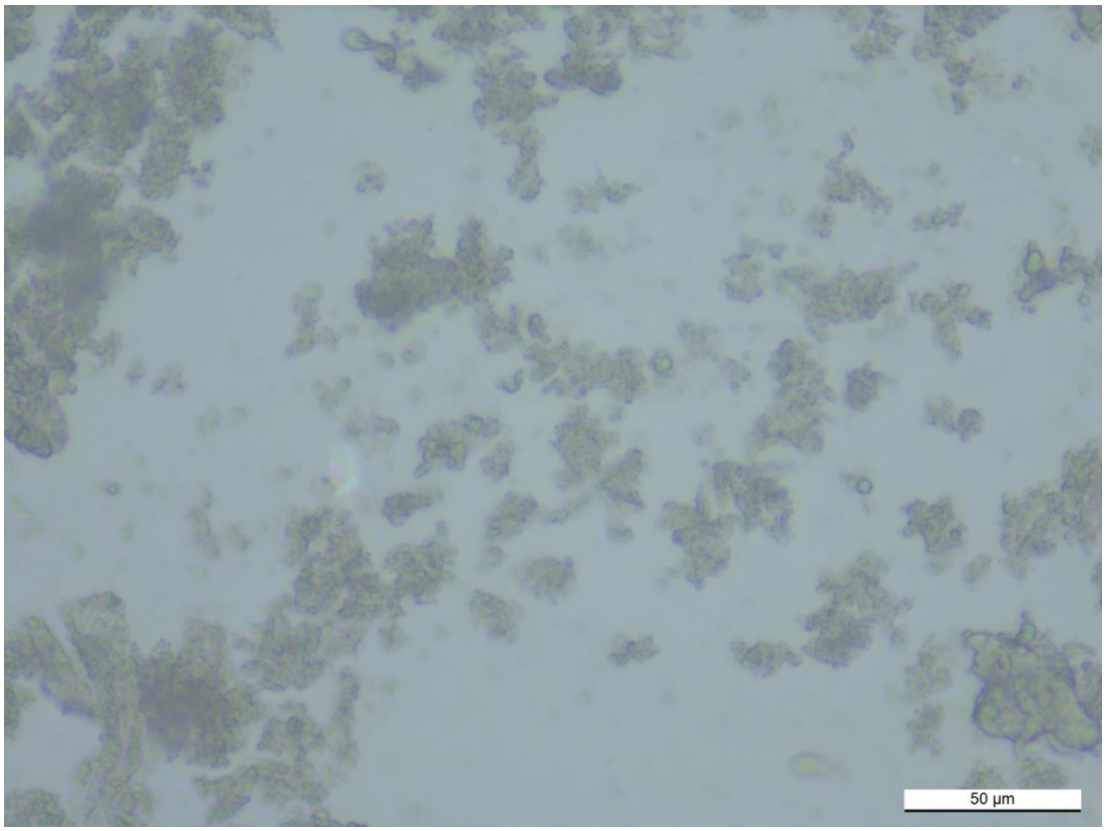

(D)

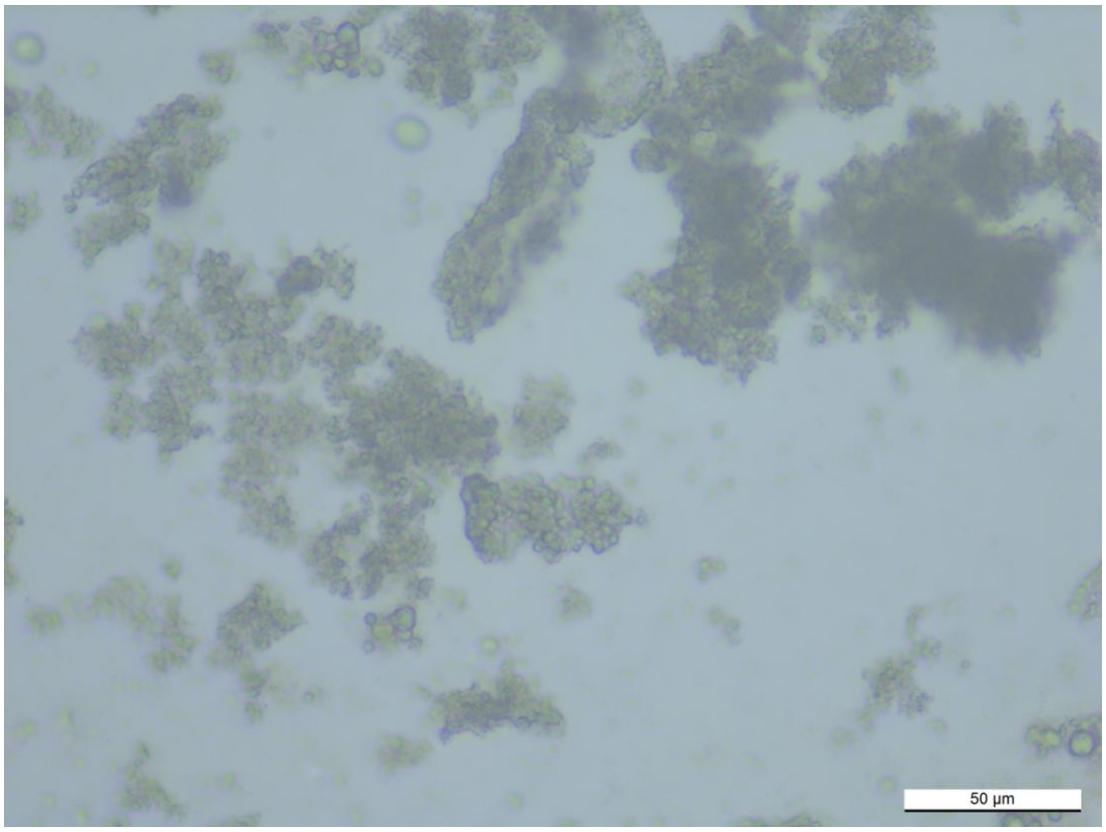

(E)

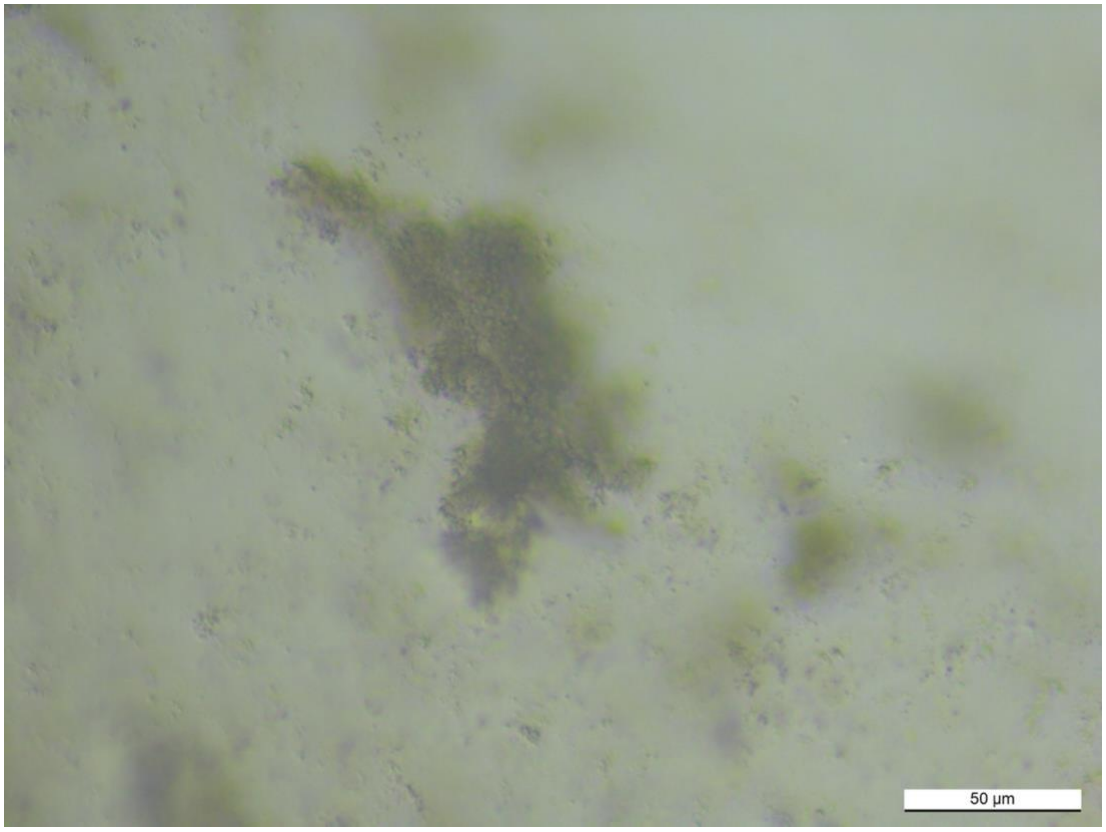

(F)

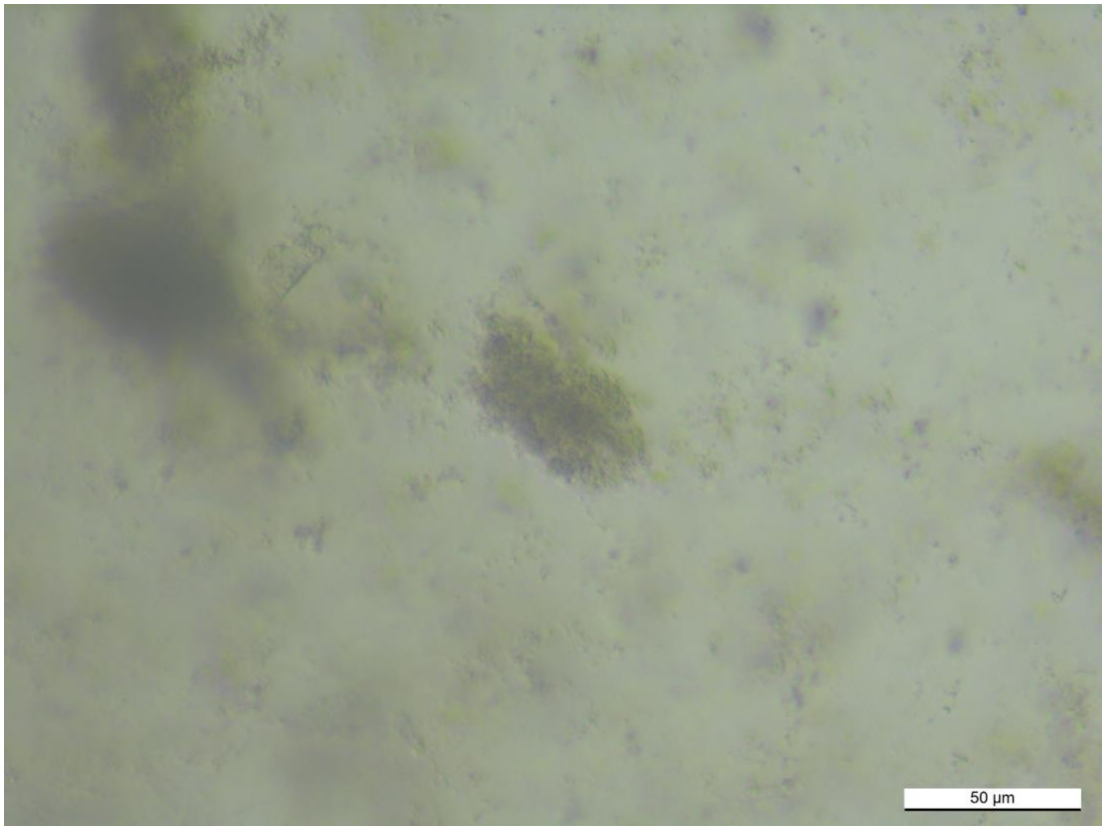

Ref: Author (2022).

All groups seem to present an aggregation behavior, which could be related to the Zeta potential of the o/w-NE. When Zp is less than 25 mV (absolute value), the attractive forces could exceed the repulsive forces, and the particles come together leading to flocculation (ROLAND *et al*., 2003). Moreover, coated droplets with proteins tend to aggregate at the pH close to their isoelectric point (MARHAMATI; RANJBAR; REZAIE, 2021). As the complexation process of chitosan and gelatin was conducted at pH 5.0, it is possible that electrostatic repulsion was inadequate to sufficiently overcome the Van der Waals and hydrophobic attractions between o/w-NE droplets.

Lemetter, Meeuse, and Zuidam (2009) discussed a similar clustering phenomenon in their study, addressing it as “polynucleated particles” and “grape coacervate”. The former was identified as several oil droplets included in a single polymer shell; the latter defined aggregates of mononucleated capsules. They also suggested that coalescence is related to the time that capsules with a fluid shell remain in close contact with each other. This statement could support the comprehension of major aggregation found for group 1:15 CS:G, once these samples present the lowest concentration of chitosan and the interaction of o/w-NE probably was more intense.

Group 1:10 CS:G exhibited well-dispersed clusters of encapsulated droplets that were attributed to the electrostatic repulsive force exerted by the positive charged CS adsorbed on the droplets of the o/w-NE and dispersed in the continuous phase. Regarding drug delivery applications, polynucleated capsules are generally considered to possess better controlled release properties than the ‘‘single core’’ microcapsules, as the former is capable of releasing the encapsulated bioactive ingredients slowly over time, whereas the latter typically release their core ingredients at one burse (WANG; ADHIKARI; BARROW, 2014).

Samples prepared with a 1:5 concentration of CS:G presented more massive agglomerates, probably derived from the superior amount of biopolymers present in the system. A high concentration of biopolymers does not allow the free movement of the molecules and restricts them in proximity, resulting in a negative effect on coacervation (TIMILSENA *et al*., 2019). Gonzalez-Monje *et al*. (2021) found a similar pattern.

OM analysis of the coacervates revealed the presence of clusters with different morphologies and dimensions. Moreover, the mixing ratio of biopolymers in the system appears as an important factor that influences the aggregation of o/w-NE droplets and the coacervation efficiency.

4.6 TEM ANALYSIS OF THE COACERVATES

TEM images showed the surface morphology of the coacervates. Some isolated spherical particles were found (Figure 22), varying from approximately 2 to 0.8 μm, considered in this work as a suggestion of successful encapsulation of copaiba oil by chitosan and gelatin complex coacervation beads. The transmission electron microscopy results confirm OM hypothesis.

Figure 22 – TEM images of complex coacervate. Scale bar of: (A) 2 μm; (B) 1 μm; (C) 0.2 μm; respectively.

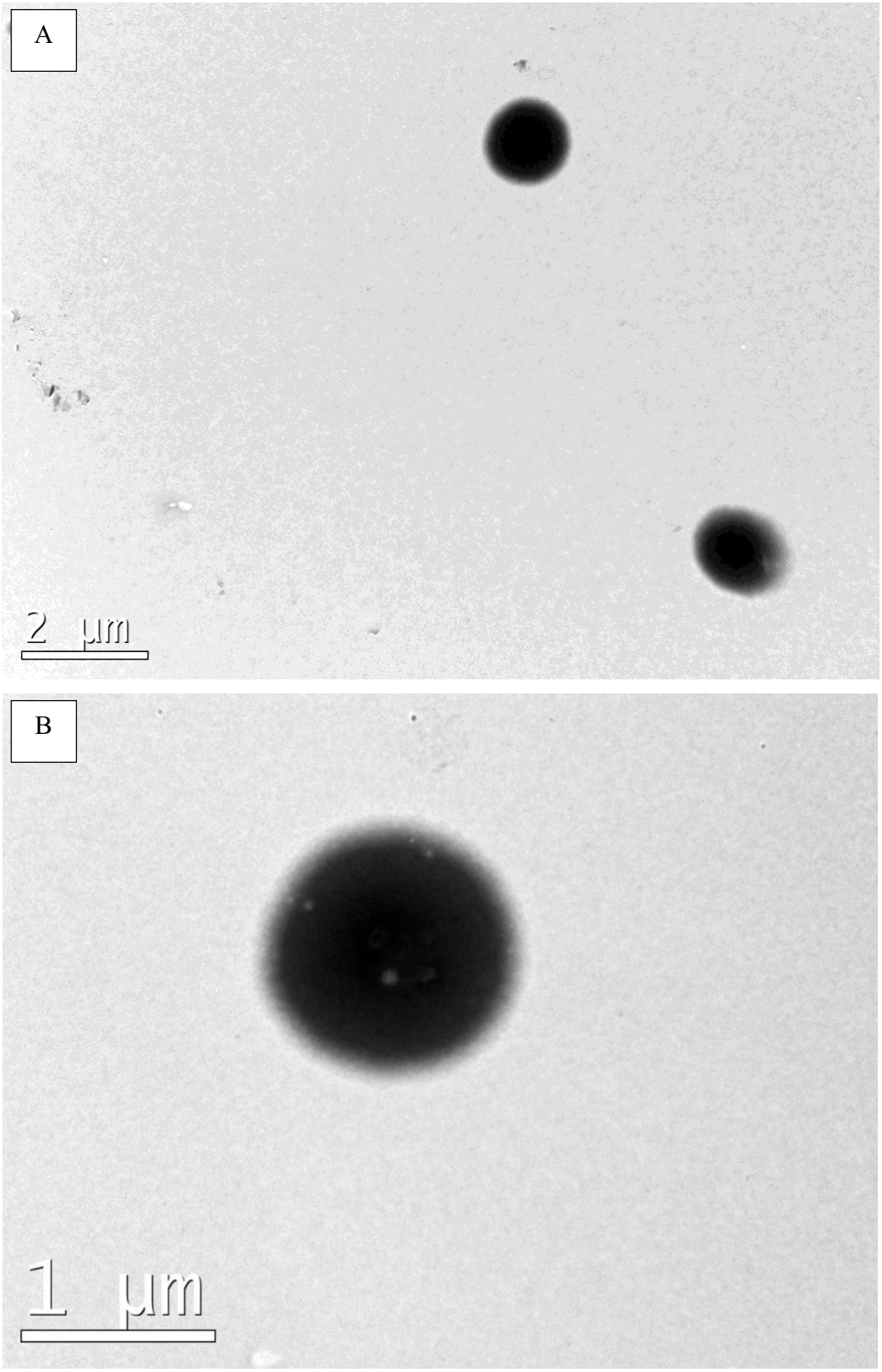

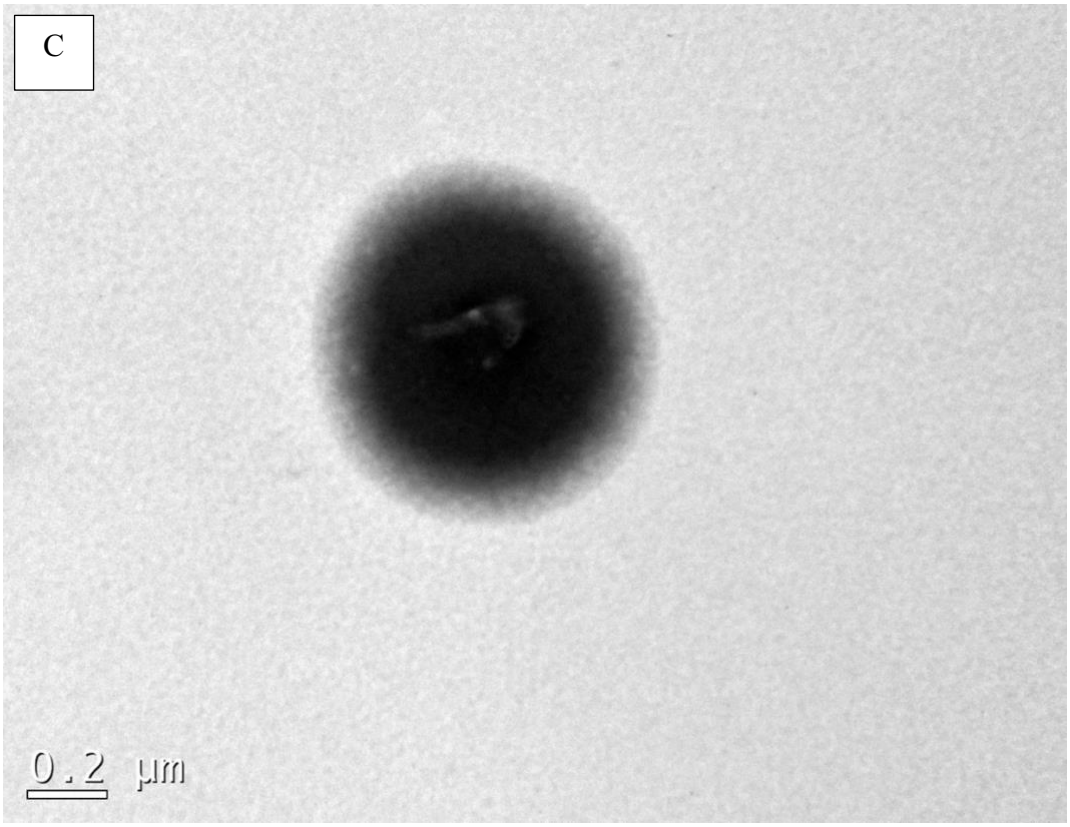

Ref: Author (2022).

4.7 PROCESS YIELD

The mixing ratio of CS:G and solution pH are the key parameters in interaction control between these two polymers. Based on Zp analysis (discussed in section 4.2), a pH of 5.0 was selected as the optimum value for the complex coacervation study. The coacervation of the nanoemulsion, previously covered with gelatin, was carried out considering 1:15, 1:10, and 1:5 CS:G mass ratio.

Under improved pH and biopolymer content ratio, coalescence occurs speedily, that is within a few minutes (PATHAK *et al*., 2017). Visual inspection of the three experimental groups revealed that, once the coacervation was induced and stirring and heating were stopped, different precipitation behavior of complexes was obtained for 1:15 CS:G. While groups with a major concentration of chitosan presented visible phase separation within a few minutes and capsules were settled at the bottom of the vial in the form of large coacervate particles after some hours, almost no precipitation of coacervates was detected for group 1:15 CS:G, as presented in Figure 23.

Figure 23 – Precipitation behavior for different groups few minutes after agitation and heating removing: (A) Group 1:10 CS:G; (B) Group 1:15 CS:G (this aspect extended until filtration process regarding yield assessment).

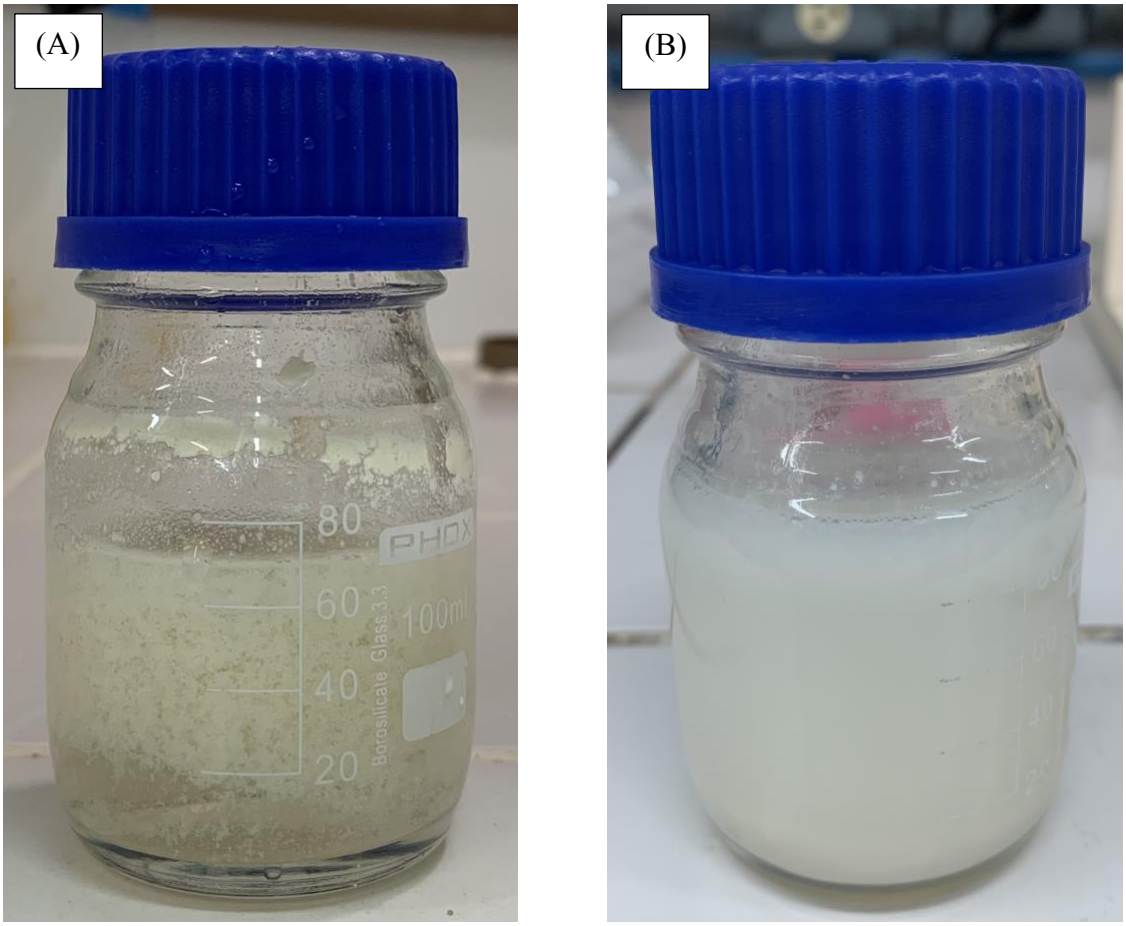

Ref: Author (2022).

Total polymers concentration in the reaction mixture is regarded by their vital role in enhancing or suppressing the complex coacervation phase separation process, as well as ionic strength (conductivity) of the solution (BUTSTRAEN; SALAÜN, 2014; DE KRUIF; WEINBRECK; DE VRIES, 2004; MU *et al*., 2022; TIMILSENA *et al*., 2019). Although very fine coacervate particles indicates a complexation phase for group 1:15 CS:G, the lower concentration of chitosan resulted in a lesser number of ions per unit of solution volume. As conductivity is based on the movements of ions in solution, and since CS is a polyelectrolyte, one possible conclusion is that this biopolymers ratio might inhibit phase separation (BUTSTRAEN; SALAÜN, 2014). Therefore, the mass ratio of biopolymers plays an important role in their binding efficiency, as the excess of one biopolymer could lead to the presence of non-neutralized charges which prevents the complexes from association with each other.

This type of interaction has been classified as soluble complexes and typically occurs in a pH range near the Ip of the protein (WAGONER; VARDHANABHUTI; FOEGEDING, 2016). In general, structures of soluble complexes have been thought to follow a core-shell theory, in which the core is primarily protein-based and polysaccharides provide an exterior shell (WAGONER; VARDHANABHUTI; FOEGEDING, 2016). However, as the purpose of this study is related to complex coacervation of copaiba oil nanoemulsion, group 1:15 CS:G was excluded from further analyzes. For the application of coacervates as wall materials in encapsulation processes, a reasonably high yield is important (SILVA; ANDRADE, 2009). Table 7 provide yield results for the systems assayed.

Table 7 – Yields for chitosan/gelatin coacervates.

	Group 1:10 CS:G	**Group 1:5 CS:G**
Yield (%)	89	88

Ref: Author (2022).

The content of coacervation is influenced by the mixing ratio of the macromolecules since the electrostatic interaction will vary depending on the amount of each macromolecule available to interact (DUBIN *et al*., 1994; PATHAK *et al*., 2017). Complex coacervation is thought to occur when the polysaccharide concentration is insufficient to cover the charged surface of the protein, resulting in polysaccharides adsorbed to the surface that bridge reactions with additional proteins (WAGONER; VARDHANABHUTI; FOEGEDING, 2016). Electrostatic binding for complex coacervation formation was already discussed for blends with CS:G 1:10 and 1:5 mixture ratios, at pH 5 (ROY *et al*., 2017).

As polysaccharides molecules are normally larger than protein ones, dilute systems provide more space in solution for adequate unfolding and interaction (GONÇALVES *et al*., 2018). Therefore, mobility would favor biopolymer chains to achieve suitable conformations for complex formation (SILVA; ANDRADE, 2009). As chitosan has a linear structure, it occupies a higher volume in the solution and could be associated with a higher coacervation yield for group 1:10 CS:G (GONÇALVES *et al*., 2018). However, once the results obtained in this test demonstrate important similarities, it was not possible to assign such correlation.

Nevertheless, the coacervation process developed in this study was mainly driven by two factors: a) CS:G mixing ratio; b) macromolecules concentration. This result is in agreement

with the literature, which highlights the aforementioned variables in combination with pH, ionic strength, and macromolecular weight as the main ones affecting complex coacervation processes (DUBIN *et al*., 1994; NAKAGAWA; NAGAO, 2012).

5 CONCLUSIONS AND OUTLOOK

5.1 CONCLUSIONS

Copaiba oil nanoemulsion synthesis and subsequent complex coacervation using chitosan and gelatin biopolymers were successfully performed. This system consists of an efficient approach to improve biomedical applications of the aforementioned oil.

Gelatin B and soy lecithin, both emulsifiers, were used as a blend to prepare copaiba oil nanoemulsion. Droplets smaller than 300 nm were achieved after homogenization at 13,000 rpm for 6 min. Although droplet sizes of gelatin-stabilized emulsions are expected to decrease linearly with increasing homogenizing time, an opposite and significant effect was observed when increasing homogenizing time over 10 minutes at 13,000 rpm, which was associated with the fast adsorption of soy lecithin on the oil droplet. The negative Zp value of o/w-NE obtained under the optimizing experimental conditions suggests that gelatin was covering the nanoparticles surface as expected.

Considering the coacervation process, chitosan, as a cationic polysaccharide, formed complexes with gelatin. A comparable charge magnitude between Zp results obtained for both biopolymers applied in this study indicate that pH 5 is the optimum point for complex coacervation tests.

The mass ratio of biopolymers played an important role in their binding efficiency, once the excess of one biopolymer was associated with the presence of non-neutralized charges preventing the complexes from association with each other. Soluble complexes were formed at a CS:G ratio of 1:15. The coacervation process developed in this study was mainly driven by two factors: CS:G mixing ratio and macromolecules concentration.

FTIR analysis confirms the incorporation of oils into the coacervate beads, as well electrostatic interactions between biopolymers applied for the complex coacervation process. Regarding coacervates morphology, polynucleated irregular-shaped microstructures were found through OM. The clustering phenomenon was associated with the Zeta potential of the o/w-NE and the concentration ratio of the chitosan-gelatin biopolymers.

5.2 OUTLOOK

For the continuation of this work, some suggestions are listed:

a) Test different types of emulsifiers and copaiba oil concentrations;
b) Assay the influence of another type of homogenizer (as ultrasound probe) in emulsion development and stability;
c) Perform turbidity measures to confirm the improved mixing ratio of biopolymers for the coacervation process;
d) Test the use of crosslinking agents for the coacervation process to evaluate stability and assess influences on the retention of the encapsulant material;
e) Investigate 1:15 CS:G group behavior for longer periods (above the 24 hours applied in this study);
f) Test encapsulation efficiency of copaiba oil by complex coacervates through high-performance liquid chromatography (HPLC);
g) Assess evidence of coacervate formation through thermogravimetric analysis (TGA).

REFERENCES

ADAMS, R. P. **Identification of essential oil components by gas chromatography/mass spectroscopy**. Ed. 4.1. Allured Pub. Corp, 2007.

AGRAWAL, P.; STRIJKERS, G. J.; NICOLAY, K. Chitosan-based systems for molecular imaging. **Advanced Drug Delivery Reviews**, v. 62, p. 42–58, 2010.

AHMADI, S. *et al*. Cinnamon extract loaded electrospun chitosan/gelatin membrane with antibacterial activity. **International Journal of Biological Macromolecules**, v. 173, p. 580–590, 15 mar. 2021.

AHMADY, A.; ABU SAMAH, N. H. A review: Gelatine as a bioadhesive material for medical and pharmaceutical applications. **International Journal of Pharmaceutics**, v. 608, p. 121037, 2021a. Elsevier B.V.

AL-MAQTARI, Q. A. *et al*. Fabrication and characterization of chitosan/gelatin films loaded with microcapsules of Pulicaria jaubertii extract. **Food Hydrocolloids**, v. 129, p. 107624, 2022.

ALVARENGA, M. O. P. *et al*. Safety and effectiveness of copaiba oleoresin (*C. reticulata ducke)* on inflammation and tissue repair of oral wounds in rats. **International Journal of Molecular Sciences**, v. 21, n. 10, p. 3568, 2020.

ARNOLD, G. *et al*. The impact of lecithin on rheology, sedimentation and particle interactions in oil-based dispersions. **Colloids and Surfaces A: Physicochemical and Engineering Aspects**, v. 418, p. 147–156, 2013.

BAKRY, A. M. *et al*. Microencapsulation of Oils: A Comprehensive Review of Benefits, Techniques, and Applications. **Comprehensive Reviews in Food Science and Food Safety**, v. 15, n. 1, p. 143–182, 2016.

BIZZO, H. R. *et al*. A set of electronic sheets for the identification and quantification of constituents of essential oils. **Quimica Nova**, v. 43, n. 1, p. 98–105, 2020.

BONAN, R. F. *et al*. In vitro antimicrobial activity of solution blow spun poly(lactic acid)/polyvinylpyrrolidone nanofibers loaded with Copaiba (*Copaifera sp.*) oil. **Materials Science and Engineering C**, v. 48, p. 372–377, 2015.

BOUCHEMAL, K. *et al*. Nano-emulsion formulation using spontaneous emulsification: Solvent, oil and surfactant optimisation. **International Journal of Pharmaceutics**, v. 280, n. 1–2, p. 241–251, 2004.

BRASIL. Ministério da Saúde. **Plantas Medicinais de Interesse ao SUS – Renisus**. Brasília, DF: Ministério da Saúde, 2021.

BUTSTRAEN, C.; SALAÜN, F. Preparation of microcapsules by complex coacervation of gum Arabic and chitosan. **Carbohydrate Polymers**, v. 99, p. 608–616, 2014.

CASCON, V.; GILBERT, B. Characterization of the chemical composition of oleoresins of *Copaifera guianensis* Desf.*, Copaifera duckei* Dwyer and *Copaifera multijuga* Hayne. **Phytochemistry**, v. 55, p. 773–778, 2000.

CEBI, N. *et al*. An evaluation of Fourier transforms infrared spectroscopy method for the classification and discrimination of bovine, porcine and fish gelatins. **Food Chemistry**, v. 190, p. 1109–1115, 2016.

CHEN, H. *et al*. Preparation, characterization, and properties of chitosan films with cinnamaldehyde nanoemulsions. **Food Hydrocolloids**, v. 61, p. 662–671, 2016.

CHOWDHURY, F. *et al*. Chronic wound-dressing chitosan-polyphenolic patch for pH responsive local antibacterial activity. **Materials Today Communications**, v. 31, p. 103310, 2022.

COPPOLA, M.; DJABOUROV, M.; FERRAND, M. Unified phase diagram of gelatin films plasticized by hydrogen bonded liquids. **Polymer**, v. 53, n. 7, p. 1483–1493, 2012.

CROISIER, F.; JÉRÔME, C. Chitosan-based biomaterials for tissue engineering. **European Polymer Journal.** Elsevier Ltd, v. 49, 780–792, 2013.

DASH, M. *et al*. Chitosan - A versatile semi-synthetic polymer in biomedical applications. **Progress in Polymer Science (Oxford).** Elsevier Ltd, v. 36, p. 981–1014, 2011.

DE KRUIF, C. G.; WEINBRECK, F.; DE VRIES, R. Complex coacervation of proteins and anionic polysaccharides. **Current Opinion in Colloid and Interface Science**, v. 9, p. 340–349, 2004.

DEBONE, H. S. *et al*. Chitosan/Copaiba oleoresin films for would dressing application. **International Journal of Pharmaceutics**, v. 555, p. 146–152, 30 jan. 2019.

DIAS, D. DE O. *et al*. Optimization of Copaiba oil-based nanoemulsions obtained by different preparation methods. **Industrial Crops and Products**, v. 59, p. 154–162, 2014.

DING, M. *et al*. Gelatin-stabilized traditional emulsions: Emulsion forms, droplets, and storage stability. **Food Science and Human Wellness**, v. 9, n. 4, p. 320–327, 1 dez. 2020.

DUBIN, P. *et al*. **Macromolecular Complexes in Chemistry and Biology Springer-Verlag**. Softcover reprint of the hardcover lst edition 1994. Springer-Verlag Berlin Heidelberg, 1994.

FERREIRA, A. S. *et al*. Influence of grape pomace extract incorporation on chitosan films properties. **Carbohydrate Polymers**, v. 113, p. 490–499, 2014.

GARCÍA-MORENO, P. J. *et al*. Biopolymers for the nanomicroencapsulation of bioactive ingredients by electrohydrodynamic processing. In: **Polymers for Food Applications**. Springer International Publishing, 2018. p. 447–479.

GIOFFRÈ, M. *et al*. Role of pH on stability and mechanical properties of gelatin films. **Journal of Bioactive and Compatible Polymers**, v. 27, n. 1, p. 67–77, jan. 2012.

GONÇALVES, N. D. *et al*. Comparison of microparticles produced with combinations of gelatin, chitosan and gum Arabic. **Carbohydrate Polymers**, v. 196, p. 427–432, 2018.

GONZÁLEZ-MONJE, P. *et al*. Encapsulation and sedimentation of nanomaterials through complex coacervation. **Journal of Colloid and Interface Science**, v. 589, p. 500–510, 2021.

HARISH PRASHANTH, K. V.; THARANATHAN, R. N. Crosslinked chitosan - Preparation and characterization. **Carbohydrate Research**, v. 341, n. 1, p. 169–173, jan. 2006.

HONG, Y. H.; MCCLEMENTS, D. J. Formation of hydrogel particles by thermal treatment of β-lactoglobulin-chitosan complexes. **Journal of Agricultural and Food Chemistry**, v. 55, n. 14, p. 5653–5660, 2007.

HOSSAIN, M. R.; MALLIK, A. K.; RAHMAN, M. M. Fundamentals of chitosan for biomedical applications. In: **Handbook of Chitin and Chitosan**. Elsevier, 2020. p. 199–230.

HOSSEINI, S. F. *et al*. Development of bioactive fish gelatin/chitosan nanoparticles composite films with antimicrobial properties. **Food Chemistry**, v. 194, p. 1266–1274, mar. 2016.

HUANG, T. *et al*. Fish gelatin modifications: A comprehensive review. **Trends in Food Science and Technology.** Elsevier Ltd, v. 86, p. 260–269, 2019.

HUO, X. *et al*. Chitosan composite microencapsulated comb-like polymeric phase change material via coacervation microencapsulation. **Carbohydrate Polymers**, v. 200, p. 602–610, nov. 2018.

HUQ, T. *et al*. Sources, production and commercial applications of fungal chitosan: A review. **Journal of Bioresources and Bioproducts.** KeAi Communications Co., v. 7, p. 85–98, 2022.

JRIDI, M. *et al*. Physical, structural, antioxidant and antimicrobial properties of gelatin-chitosan composite edible films. **International Journal of Biological Macromolecules**, v. 67, p. 373–379, 2014.

KALANTARI, K. *et al*. Biomedical applications of chitosan electrospun nanofibers as a green polymer – Review. **Carbohydrate Polymers.** Elsevier Ltd, v. 207, p. 588–600, 2019.

KANG, M. K.; DAI, J.; KIM, J. C. Ethylcellulose microparticles containing chitosan and gelatin: PH-dependent release caused by complex coacervation. **Journal of Industrial and Engineering Chemistry**, v. 18, n. 1, p. 355–359, 2012.

KARIM, A. A.; BHAT, R. Fish gelatin: properties, challenges, and prospects as an alternative to mammalian gelatins. **Food Hydrocolloids**, v. 23, p. 563–576, 2009.

KOŁODZIEJSKA, M. *et al*. Chitosan as an underrated polymer in modern tissue engineering. **Nanomaterials**, v. 11, n. 11, p. 3019, nov. 2021. MDPI AG.

LAMMARI, N. *et al*. Plant oils: From chemical composition to encapsulated form use. **International Journal of Pharmaceutics.** Elsevier B.V., v. 601, p. 120538, 2021.

LEANDRO, L. M. *et al*. Chemistry and biological activities of terpenoids from copaiba (*Copaifera spp.)* oleoresins. **Molecules**, v. 17, n. 4, p. 3866-3889, 2012. MDPI AG.

LEMETTER, C. Y. G.; MEEUSE, F. M.; ZUIDAM, N. J. Control of the morphology and the size of complex coacervate microcapsules during scale-up. **AIChE Journal**, v. 55, n. 6, p. 1487–1496, jun. 2009.

LI, D. *et al*. Superior environmental stability of gelatin/CMC complex coacervated microcapsules via chitosan electrostatic modification. **Food Hydrocolloids**, v. 124, p. 107341, 2022.

LI, X. *et al*. Gelatin films incorporated with thymol nanoemulsions: Physical properties and antimicrobial activities. **International Journal of Biological Macromolecules**, v. 150, p. 161–168, 2020.

LIANG, H. *et al*. Fabrication of tragacanthin gum-carboxymethyl chitosan bio-nanocomposite wound dressing with silver-titanium nanoparticles using freeze-drying method. **Materials Chemistry and Physics**, v. 279, p. 125770, mar. 2022.

LIMA, S. R. M. *et al*. In vivo and in vitro Studies on the Anticancer Activity of *Copaifera multijuga* Hayne and its Fractions. **Phytotherapy Research**, v. 17, n. 9, p. 1048–1053, nov. 2003.

LIU, D. *et al*. Collagen and gelatin. **Annual Review of Food Science and Technology.** Annual Reviews Inc., v. 6, n. 1, p. 527-557, 2015.

LIU, H. *et al*. Chitosan kills bacteria through cell membrane damage. **International Journal of Food Microbiology**, v. 95, n. 2, p. 147–155, set. 2004.

LIU, Y. *et al*. Preparation and characterization of gelatin/chitosan/3-phenylacetic acid food-packaging nanofiber antibacterial films by electrospinning. **International Journal of Biological Macromolecules**, v. 169, p. 161–170, 2021.

LOO, H. L. *et al*. Application of chitosan-based nanoparticles in skin wound healing. **Asian Journal of Pharmaceutical Sciences**, v. 17, n. 3, p. 299-332, 2022.

LOPES ROCHA CORREA, V. *et al*. Melatonin loaded lecithin-chitosan nanoparticles improved the wound healing in diabetic rats. **International Journal of Biological Macromolecules**, v. 162, p. 1465–1475, 2020.

LU, B. *et al*. Healing of skin wounds with a chitosan-gelatin sponge loaded with tannins and platelet-rich plasma. **International Journal of Biological Macromolecules**, v. 82, p. 884–891, jan. 2016.

LUCCA, L. G. *et al*. Determination of β-caryophyllene skin permeation/retention from crude copaiba oil (*Copaifera multijuga* Hayne) and respective oil-based nanoemulsion using a novel HS-GC/MS method. **Journal of Pharmaceutical and Biomedical Analysis**, v. 104, p. 144–148, 2015.

MA, Y. *et al*. Chitosan membrane dressings toughened by glycerol to load antibacterial drugs for wound healing. **Materials Science and Engineering C**, v. 81, p. 522–531, 2017.

MAGANTI, N. *et al*. Structure-process-property relationship of biomimetic chitosan-based nanocomposite scaffolds for tissue engineering: Biological, physico-chemical, and mechanical functions. **Advanced Engineering Materials**, v. 13, n. 3, mar. 2011.

MARANGON, C. A. *et al*. Chitosan/gelatin/copaiba oil emulsion formulation and its potential on controlling the growth of pathogenic bacteria. **Industrial Crops and Products**, v. 99, p. 163–171, 2017.

MARHAMATI, M.; RANJBAR, G.; REZAIE, M. Effects of emulsifiers on the physicochemical stability of Oil-in-water Nanoemulsions: A critical review. **Journal of Molecular Liquids.** Elsevier B.V., v. 340, p. 117218, 2021.

MATI-BAOUCHE, N. *et al*. Chitosan as an adhesive. **European Polymer Journal.** Elsevier Ltd, v. 60, p. 198–212, 2014.

MAYYA, K. S.; BHATTACHARYYA, A.; ARGILLIER, J. F. Micro-encapsulation by complex coacervation: Influence of surfactant. **Polymer International**, v. 52, n. 4, p. 644–647, 2003.

MCCLEMENTS, D. J.; JAFARI, S. M. Improving emulsion formation, stability and performance using mixed emulsifiers: A review. **Advances in Colloid and Interface Science.** Elsevier B.V., v. 251, p. 55–79, 2018.

MENDES DE LACERDA LEITE, G. *et al*. Pharmacological and toxicological activities of α-humulene and its isomers: A systematic review. **Trends in Food Science and Technology.** Elsevier Ltd, v. 115, p. 255–274, 2021.

MENEZES, A. C. DOS S. *et al*. Anti-inflammatory and wound healing effect of Copaiba oleoresin on the oral cavity: A systematic review. **Heliyon.** Elsevier Ltd, v. 8, n. 2, p. e08993, 2022. http://dx.doi.org/10.1016/j.heliyon.2022.e08993.

MU, H. *et al*. Microencapsulation of algae oil by complex coacervation of chitosan and modified starch: Characterization and oxidative stability. **International Journal of Biological Macromolecules**, v. 194, p. 66–73, 2022.

MUXIKA, A. *et al*. Chitosan as a bioactive polymer: Processing, properties and applications. **International Journal of Biological Macromolecules.** Elsevier B.V., v. 105, p. 1358–1368, 2017.

NAKAGAWA, K.; NAGAO, H. Microencapsulation of oil droplets using freezing-induced gelatin-acacia complex coacervation. **Colloids and Surfaces A: Physicochemical and Engineering Aspects**, v. 411, p. 129–139, 5 out. 2012.

NAKASHIMA, K. K.; VIBHUTE, M. A.; SPRUIJT, E. Biomolecular chemistry in liquid phase separated compartments. **Frontiers in Molecular Biosciences.** Frontiers Media S.A., v. 6, Article 21, 2019.

NIEHUES, E.; QUADRI, M. G. N. Spinnability, morphology and mechanical properties of gelatins with different bloom index. **Brazilian Journal of Chemical Engineering**, v. 34, n. 1, p. 253–261, 2017.

NIGRO, F. *et al*. Development, characterization and in vitro toxicity evaluation of nanoemulsion-loaded hydrogel based on copaiba oil and coenzyme Q10. **Colloids and Surfaces A: Physicochemical and Engineering Aspects**, v. 586, p. 124132, 2020.

NORCINO, L. B. *et al*. Pectin films loaded with copaiba oil nanoemulsions for potential use as bio-based active packaging. **Food Hydrocolloids**, v. 106, p. 105862, 2020.

ORF, M. *et al*. Thermochemical properties of sesquiterpenes in natural products by correlation gas chromatography: Application to bergamotene oil. **Journal of Chemical Thermodynamics**, v. 126, p. 128–136, 2018.

ORYAN, A.; SAHVIEH, S. Effectiveness of chitosan scaffold in skin, bone and cartilage healing. **International Journal of Biological Macromolecules.** Elsevier B.V., v. 104, p. 1003–1011, 2017.

PAKIZEH, M.; MORADI, A.; GHASSEMI, T. Chemical extraction and modification of chitin and chitosan from shrimp shells. **European Polymer Journal.** Elsevier Ltd, v. 159, p. 110709, 2021.

PARISOTTO-PETERLE, J. *et al*. Healing activity of hydrogel containing nanoemulsified β-caryophyllene. **European Journal of Pharmaceutical Sciences**, v. 148, p. 105318, 2020.

PATHAK, J. *et al*. Complex coacervation in charge complementary biopolymers: Electrostatic versus surface patch binding. **Advances in Colloid and Interface Science.** Elsevier B.V., v. 250, p. 40–53, 2017.

PELISSARI, F. M. *et al*. Antimicrobial, mechanical, and barrier properties of cassava starch-chitosan films incorporated with oregano essential oil. **Journal of Agricultural and Food Chemistry**, v. 57, n. 16, p. 7499–7504, 2009.

PEREDA, M. *et al*. Chitosan-gelatin composites and bi-layer films with potential antimicrobial activity. **Food Hydrocolloids**, v. 25, n. 5, p. 1372–1381, jul. 2011.

PÉREZ CÓRDOBA, L. J.; SOBRAL, P. J. A. Physical and antioxidant properties of films based on gelatin, gelatin-chitosan or gelatin-sodium caseinate blends loaded with nanoemulsified active compounds. **Journal of Food Engineering**, v. 213, p. 47–53, 2017.

PRATA, A. S.; GROSSO, C. R. F. Production of microparticles with gelatin and chitosan. **Carbohydrate Polymers**, v. 116, p. 292–299, 2015.

QIAO, C. *et al*. Molecular interactions in gelatin/chitosan composite films. **Food Chemistry**, v. 235, p. 45–50, 2017.

QIN, S.; LI, H.; HU, C. Thermal properties and morphology of chitosan/gelatin composite shell microcapsule via multi-emulsion. **Materials Letters**, v. 291, p. 129475, 2021.

RAZA, Z. A. *et al*. Recent developments in chitosan encapsulation of various active ingredients for multifunctional applications. **Carbohydrate Research**, v. 492, p. 108004, 2020.

REYES, L. M.; LANDGRAF, M.; SOBRAL, P. J. A. Gelatin-based films activated with red propolis ethanolic extract and essential oils. **Food Packaging and Shelf Life**, v. 27, p. 100607, 2021.

REZAEI, F. S. *et al*. **Chitosan films and scaffolds for regenerative medicine applications: A review**. **Carbohydrate Polymers.** Elsevier Ltd, v. 273, p. 118631, 2021.

RICARDO, L. M. *et al*. Evidence of traditionality of Brazilian medicinal plants: The case studies of *Stryphnodendron adstringens* (Mart.) Coville (barbatimão) barks and *Copaifera* spp. (copaíba) oleoresin in wound healing. **Journal of Ethnopharmacology**, v. 219, p. 319–336, 2018.

ROLAND, I. *et al*. Systematic characterization of oil-in-water emulsions for formulation design. **International Journal of Pharmaceutics**, v. 263, n. 1–2, p. 85–94, 2003.

ROY, J. C. *et al*. Surface behavior and bulk properties of aqueous chitosan and type-B gelatin solutions for effective emulsion formulation. **Carbohydrate Polymers**, v. 173, p. 202–214, 2017.

ROY, J. C. *et al*. Influence of process parameters on microcapsule formation from chitosan—Type B gelatin complex coacervates. **Carbohydrate Polymers**, v. 198, p. 281–293, 2018.

SEGTNAN, V. H.; ISAKSSON, T. Temperature, sample and time dependent structural characteristics of gelatine gels studied by near infrared spectroscopy. **Food Hydrocolloids**, v. 18, n. 1, p. 1–11, 2004.

SHAH, P. R.; GAITONDE, U. N.; GANESH, A. Influence of soy-lecithin as bio-additive with straight vegetable oil on CI engine characteristics. **Renewable Energy**, v. 115, p. 685–696, 2018.

SILVA, A. O. *et al*. Chitosan as a matrix of nanocomposites: A review on nanostructures, processes, properties, and applications. **Carbohydrate Polymers.** Elsevier Ltd, v. 272, p. 118472, 2021.

SILVA, M. C.; ANDRADE, C. T. Evaluating Conditions for the Formation of. **Polímeros**, v. 19, p. 133–137, 2009.

SINGH, N.; SHEIKH, J. Novel Chitosan-Gelatin microcapsules containing rosemary essential oil for the preparation of bioactive and protective linen. **Industrial Crops and Products**, v. 178, 2022.

SINGH, V. K. *et al*. Development of soy lecithin based novel self-assembled emulsion hydrogels. **Journal of the Mechanical Behavior of Biomedical Materials**, v. 55, p. 250–263, 2016.

SIVASHANKARI, P. R.; PRABAHARAN, M. Prospects of chitosan-based scaffolds for growth factor release in tissue engineering. **International Journal of Biological Macromolecules**, v. 93, p. 1382–1389, 2016.

SU, K.; WANG, C. Recent advances in the use of gelatin in biomedical research. **Biotechnology Letters.** Kluwer Academic Publishers, v. 37, p. 2139–2145, nov. 2015.

SUH, J.-K. F.; MATTHEW, H. W. T. Application of chitosan-based polysaccharide biomaterials in cartilage tissue engineering: a review. **Biomaterials**, v. 21, p. 2589–2598, 2000.

TANG, S. Y. *et al*. Formulation development and optimization of a novel Cremophore EL-based nanoemulsion using ultrasound cavitation. **Ultrasonics Sonochemistry**, v. 19, n. 2, p. 330–345, 2012.

TEIXEIRA, F. B. *et al*. Copaiba oil-resin (*Copaifera reticulata* Ducke) modulates the inflammation in a model of injury to rats' tongues. **BMC Complementary and Alternative Medicine**, v. 17, n. 1, 2017.

TERZIOĞLU, P. Electrospun Chitosan/Gelatin/Nano-CaCO3 Hybrid Nanofibers for Potential Tissue Engineering Applications. **Journal of Natural Fibers**, v. 18, n. 8, p. 1207–1216, 2021.

TIMILSENA, Y. P. *et al*. Advances in microencapsulation of polyunsaturated fatty acids (PUFAs)-rich plant oils using complex coacervation: A review. **Food Hydrocolloids.** Elsevier B.V., v. 69, p. 369–381, 2017.

TIMILSENA, Y. P. *et al*. Complex coacervation: Principles, mechanisms and applications in microencapsulation. **International Journal of Biological Macromolecules.** Elsevier B.V., v. 121, p. 1276–1286, jan. 2019.

VALENCIA, M. S. *et al*. Characterization of curcumin-loaded lecithin-chitosan bioactive nanoparticles. **Carbohydrate Polymer Technologies and Applications**, v. 2, p. 100119, 2021.

VATER, C. *et al*. Cytotoxicity of lecithin-based nanoemulsions on human skin cells and ex vivo skin permeation: Comparison to conventional surfactant types. **International Journal of Pharmaceutics**, v. 566, p. 383–390, jul. 2019.

VATER, C. *et al*. Changes in skin barrier function after repeated exposition to phospholipid-based surfactants and sodium dodecyl sulfate in vivo and corneocyte surface analysis by atomic force microscopy. **Pharmaceutics**, v. 13, n. 4, 2021.

VATER, C. *et al*. Lecithin-based nanoemulsions of traditional herbal wound healing agents and their effect on human skin cells. **European Journal of Pharmaceutics and Biopharmaceutics**, v. 170, p. 1–9, jan. 2022.

VEIGA, V. F. *et al*. Chemical composition and anti-inflammatory activity of copaiba oils from *Copaifera cearensis* Huber ex Ducke, *Copaifera reticulata* Ducke and *Copaifera multijuga* Hayne- A comparative study. **Journal of Ethnopharmacology**, v. 112, n. 2, p. 248–254, 13 jun. 2007.

VIEIRA, R. C. *et al*. Influência do óleo de *Copaifera langsdorffii* no reparo de ferida cirúrgica em presença de corpo estranho. **Pesq. Vet. Bras**, p. 358-366, 2008.

VORON'KO, N. G. *et al*. The chitosan-gelatin (bio)polyelectrolyte complexes formation in an acidic medium. **Carbohydrate Polymers**, v. 138, p. 265–272, 15 mar. 2016.

WAGONER, T.; VARDHANABHUTI, B.; FOEGEDING, E. A. Designing Whey Protein-Polysaccharide Particles for Colloidal Stability. **Annual Review of Food Science and Technology.** Annual Reviews Inc., v. 7, n. 1, p. 93-116, 2016.

WANG, B.; ADHIKARI, B.; BARROW, C. J. Optimisation of the microencapsulation of tuna oil in gelatin-sodium hexametaphosphate using complex coacervation. **Food Chemistry**, v. 158, p. 358–365, 2014.

WANG, X. Y.; HEUZEY, M. C. Pickering emulsion gels based on insoluble chitosan/gelatin electrostatic complexes. **RSC Advances**, v. 6, n. 92, p. 89776–89784, 2016.

WANG, X. Y.; WANG, C. S.; HEUZEY, M. C. Complexation of chitosan and gelatin: From soluble complexes to colloidal gel. **International Journal of Polymeric Materials and Polymeric Biomaterials**, v. 65, n. 2, p. 96–104, jan. 2016.

XIONG, Y. *et al*. Incorporation of salmon bone gelatine with chitosan, gallic acid and clove oil as edible coating for the cold storage of fresh salmon fillet. **Food Control**, v. 125, p. 107994, jul. 2021.

XU, J. *et al*. Characteristics and bioactive functions of chitosan/gelatin-based film incorporated with ε-polylysine and astaxanthin extracts derived from by-products of shrimp (Litopenaeus vannamei). **Food Hydrocolloids**, v. 100, p. 105436, mar. 2020.

XUE, J.; DAVIDSON, P. M.; ZHONG, Q. Inhibition of *Escherichia coli* O157:H7 and *Listeria monocytognes* growth in milk and cantaloupe juice by thymol nanoemulsions prepared with gelatin and lecithin. **Food Control**, v. 73, p. 1499–1506, 1 mar. 2017.

XUE, J.; ZHONG, Q. Blending lecithin and gelatin improves the formation of thymol nanodispersions. **Journal of Agricultural and Food Chemistry**, v. 62, n. 13, p. 2956–2962, 2014.

YI, H. *et al.* Biofabrication with chitosan. **Biomacromolecules**, v. 6, n. 6, p. 2881-2894, nov. 2005.

YONG, A. P.; ISLAM, MD. A.; HASAN, N. The Effect of pH and High-Pressure Homogenization on Droplet Size. **International Journal of Engineering Materials and Manufacture**, v. 2, n. 4, p. 110–122, 2017.

ZHANG, T. *et al*. Effects of surfactant type and preparation pH on the droplets and emulsion forms of fish oil-loaded gelatin/surfactant-stabilized emulsions. **LWT - Food Science and Technology**, v. 117, p. 108654, jan. 2020a.

ZHANG, T. *et al*. Fish oil-loaded emulsions stabilized by synergetic or competitive adsorption of gelatin and surfactants on oil/water interfaces. **Food Chemistry**, v. 308, p. 125597, mar. 2020b.

ZHANG, T. *et al*. Commercial cold-water fish skin gelatin and bovine bone gelatin: Structural, functional, and emulsion stability differences. **LWT - Food Science and Technology**, v. 125, p. 109207, 2020c.

ZHANG, T. *et al*. Gelatins as emulsifiers for oil-in-water emulsions: Extraction, chemical composition, molecular structure, and molecular modification. **Trends in Food Science and Technology.** Elsevier Ltd, v. 106, p. 113-131, 2020d.